Naval Research Laboratory
Washington, DC 20375-5000

NRL Memorandum Report 6347

Transformations of Gaussian Light Beams Caused by Reflection in FEL Resonators

S. RIYOPOULOS

Science Applications Intl. Corp.
McLean, VA 22102

C. M. TANG AND P. SPRANGLE

Plasma Theory Branch
Plasma Physics Division

October 27, 1988

SECURITY CLASSIFICATION OF THIS PAGE

AD-A202 472

REPORT DOCUMENTATION PAGE

Form Approved OMB No 0704-0188

1a REPORT SECURITY CLASSIFICATION: UNCLASSIFIED	1b RESTRICTIVE MARKINGS
2a SECURITY CLASSIFICATION AUTHORITY	3 DISTRIBUTION AVAILABILITY OF REPORT: Approved for public release; distribution unlimited.
2b DECLASSIFICATION / DOWNGRADING SCHEDULE	
4 PERFORMING ORGANIZATION REPORT NUMBER(S): NRL Memorandum Report 6347	5 MONITORING ORGANIZATION REPORT NUMBER(S)
6a NAME OF PERFORMING ORGANIZATION: Naval Research Laboratory; 6b OFFICE SYMBOL (If applicable): Code 4790	7a NAME OF MONITORING ORGANIZATION
6c ADDRESS (City, State, and ZIP Code): Washington, DC 20375-5000	7b ADDRESS (City, State, and ZIP Code)
8a NAME OF FUNDING / SPONSORING ORGANIZATION: Strategic Defense Initiative Organization; 8b OFFICE SYMBOL (If applicable)	9 PROCUREMENT INSTRUMENT IDENTIFICATION NUMBER
8c ADDRESS (City, State, and ZIP Code): Washington, DC 20301-7100	10 SOURCE OF FUNDING NUMBERS: PROGRAM ELEMENT NO: 63221C; PROJECT NO: 7-D4039; TASK NO; WORK UNIT ACCESSION NO

11 TITLE (Include Security Classification)

Transformations of Gaussian Light Beams Caused by Reflection in FEL Resonators

12 PERSONAL AUTHOR(S)

Riyopoulos,* S., Tang, C.M. and Sprangle, P.

13a TYPE OF REPORT	13b TIME COVERED	14 DATE OF REPORT (Year, Month, Day)	15 PAGE COUNT
Interim	FROM _____ TO _____	1988 October 27	75

16 SUPPLEMENTARY NOTATION

*Science Application Intl. Corp., McLean, VA 22102

17 COSATI CODES			18 SUBJECT TERMS (Continue on reverse if necessary and identify by block number)
FIELD	GROUP	SUB-GROUP	FEL oscillators; Optical resonators; Reflection matrix

19 ABSTRACT (Continue on reverse if necessary and identify by block number)

The transformation of Gaussian radiation beams caused by reflection off mirrors is an important issue for FELs operating as oscillators. The reflected radiation from a single incident Gaussian mode will contain other modes due to the finite mirror size, the deflection of the beam and mismatches in the curvature. A method for analytic computation of the reflection matrix is developed by taking the convolution of the source function at the surface of the mirror with the paraxial propagator. The mirror surface that reflects spherical incoming wavefronts into spherical outgoing is determined analytically. Integral expressions for the reflection coefficients R_{pq}^{mn} for any incoming mode u_{mn} into the outgoing u_{pq} are obtained as functions of the deflection angle ϕ, the reflected beam waist w_0 and the mirror size. Analytic expansions of the reflection matrix in powers of the diffraction angle $\theta_d << 1$ are then obtained in both Hermite and Laguerre representations. The

(Continues)

20 DISTRIBUTION / AVAILABILITY OF ABSTRACT	21 ABSTRACT SECURITY CLASSIFICATION
☒ UNCLASSIFIED/UNLIMITED ☐ SAME AS RPT ☐ DTIC USERS	UNCLASSIFIED
22a NAME OF RESPONSIBLE INDIVIDUAL: P. Sprangle	22b TELEPHONE (Include Area Code): (202) 767-3493; 22c OFFICE SYMBOL: Code 4790

DD Form 1473, JUN 86 Previous editions are obsolete SECURITY CLASSIFICATION OF THIS PAGE

S/N 0102-LF-014-6603

19. ABSTRACTS (Continued)

cross-coupling among vector components of the radiation field, caused by the curvature of the mirror surface, is included. It is shown that the lowest order contribution to the off-diagonal matrix elements is caused by the finite mirror size. The effects of the mirror curvature and the deflection of the light beam enter the reflection matrix as first order corrections in

CONTENTS

TRANSFORMATIONS OF GAUSSIAN LIGHT BEAMS CAUSED BY REFLECTION IN FEL RESONATORS

I. INTRODUCTION

Free Electron Lasers (FELs) operating as oscillators[1-7] require the trapping of light pulses between systems of mirrors (resonators).[8,9] These pulses are repeatedly amplified via synchronous interaction with electron pulses passing through the wiggler. The radiation produced by the stimulated emission is confined within a narrow cone along the beam axis. Therefore, the vector potential can be represented as a superposition of Gaussian modes. Those are the free space eigenmodes $A_{mn}(r) = e_{mn}A_{mn}(r)e^{ikz}$ where e_{mn} is the polarization vector, of the paraxial equation,[10]

$$\nabla_{\perp}^2 A - 2ik \frac{\partial A}{\partial z} = 0. \qquad (1)$$

Equation (1) is the $k_{\perp} << k = \omega/c$ limit of the exact wave equation. The simplest oscillator configuration is that of an open resonator with two opposed identical mirrors. The vacuum eigenmodes for this arrangement are also expressed in terms of the paraxial eigenmodes. Their detailed structure can be described in terms of either Gaussian-Hermite functions in rectangular coordinates, or Laguerre functions in polar coordinates. In both representations all the eigenmodes with given wave number k are characterized by two independent parameters: the waist $w = (2b/k)^{1/2}$ and the curvature of the wave front $1/R = z/(z^2 + b^2)$, where z is the distance from the waist position and b is the Rayleigh length (Fig. 1).

The electron beam is an optically active medium that alters the characteristic parameters of the radiation after each passage. During the build-up period the modal content and the structure of the light pulses inside the oscillator will change. A numerical method has been developed recently optimizing the representation for the amplified radiation. In the source dependent expansion[11,12] the waist size and the curvature of the elected modal basis is tailored according to the driving source term. That

Manuscript approved August 8, 1988.

minimizes the number of modes required to describe the light beam. In general, the curvature and waist size of these modes does not match the curvature and waist of the vacuum eigenmodes for the resonator. Therefore, the transfer matrix for a given mirror must be known for arbitrary incoming modes. This need stems from computational as well as physical reasons. The knowledge of the cavity reflection matrix **R**, together with the gain matrix **G** through the wiggler, is necessary in determining the potential for steady state operation.

The study of the reflection matrix must include the effects of deflecting the light beam, in addition to finite mirror size and curvature mismatches. During high power operation, grazing mirror incidence may be necessary to avoid exceeding the dielectric breakdown limit for the reflecting surface. Also, in case of a high per-pass gain with optical guiding, the spot size for the reflected radiation could be much larger than the incoming. In two mirror resonators, the reflected radiation could then damage the wiggler. Therefore, ring resonators, including three or more mirrors, must be employed for the deflection and recirculation of the light pulses.

We are interested in cases when the reflected radiation remains focused along some direction $\hat{z}_o$ making an angle ϕ with the incoming $\hat{z}_i$. Then the reflected vector potential will also be expandable in free space eigenmodes $A_{pq}(r_o)$ of the paraxial equation in the new direction. The mirror surface generating focused reflection in the desired direction can not be arbitrary but must be appropriately defined. The angle of deflection ϕ will enter the equation defining the mirror surface. The other surface parameter, namely the curvature $1/R_m$, is a free parameter. It determines the curvature $1/R_o$ for the outgoing modes given the curvature $1/R_i$ of the incoming modes. In case of reflection by an arbitrary surface,

the scattered radiation cannot, in general, be covered by the paraxial modes that do not form a complete set in three dimensions.

A single incident mode $A_{mn}(r_i)$ will, in general, be partially reflected into different modes $A_{pq}(r_o)$ where $(m,n)\neq(p,q)$. This is caused by the deflection of the light beam, the finite size of the mirror and the curvature mismatches. Reflection into other modes will affect the interaction between the electron beam and the radiation in a number of ways. First, the rms radius of the light beam will change, affecting the matching beam condition. Second, the light pulse will spread axially because of dispersion among different modes, since the phase velocity depends on the modal number (m,n). Third, different phase shifts among the various modes during reflection may render these modes out of phase after a number of bouncings off the resonator. For the above reasons the fraction of radiation scattered into other modes will contribute to the losses in FEL oscillators.

The method for obtaining the reflection matrix is outlined in Sec. II. The definition of the appropriate mirror surface is given in Sec. III. In Sec. IV the integral expressions for the matrix elements are derived. An analytic expansion in powers of a small parameter (of the order of the diffraction angle) is given in the same section. Some limiting cases are examined in Sec. V. In Sec. VI the reflection of the fundamantal mode (0,0) is studied in detail. Section VII deals with cross-coupling effects among the vector components of the radiation.

II. OUTLINE OF THE METHOD

The free space eigenmodes $A_{mn}(r)$ of the paraxial wave equation have the general form

$$A_{mn}(r) = \frac{u_{mn}(r;W)}{\left(1 + \frac{z^2}{b^2}\right)^{1/2}} e^{i\left[kz + \frac{k(x^2 + y^2)}{2R(z)}\right]} e^{i\delta_{mn}(z)} . \qquad (2)$$

The first exponential in (2) contains the rapidly varying phase on the wavelength scale $\lambda = 2\pi/k$. The wavefronts are spherical with radius of curvature $R(z)$ given by $1/R(z) = z/(z^2 + b^2)$. The spot size of the radiation envelope is $W(z) = w(1 + z^2/b^2)^{1/2}$, where $w = (2b/k)^{1/2}$ is the waist, and the distance z is measured from the position of the waist. The amplitude squared of the mode drops by 1/2 over a distance equal to the Rayleigh length b (also known as confocal parameter). Most of the radiation is confined within a cone parametrized by the diffraction angle $\theta_d = W/z \simeq (\lambda/b\pi)^{1/2}$. The structure of the amplitude profile $u_{mn}(r;W)$ depends on the elected coordinate system. $u_{mn}(r;W)$ contains the slow spatial variation equivalent to a small wave number perpendicular to the z-direction. Higher modes correspond to an increasing effective $k_\perp$, producing the slow phase shift expressed by the term exp $[i\delta_{mn}(z)]$. For a given k, the mode is completely defined by the two independent parameters R and w (or any combination of two out of the four quantities R, w, z and b).

The geometry of the reflection is illustrated in Fig. 2. The subscripts i and o denote the coordinate system used for expressing incoming and outgoing modes. r_i is defined with the $\hat{z}_i$ axis along the direction of incidence and r_o has the $\hat{z}_o$ axis along the direction of reflection. The origins are displaced from the mirror center by l_i and l_o respectively, where l_i is the distance of the minimum waist w_i for the

incoming radiation and l_o is the distance of the minimum waist w_o for the reflected mode. A third coordinate system r_s with the origin at the mirror center and $\hat{z}_m$ aligned with the mirror axis will be useful in the computations. Underlined quantities $\underline{r}_i$, $\underline{r}_o$ and $\underline{r}_s$ stand for the mirror surface coordinates in each reference frame. The transformations among the various frames are defined by

$$x_i = x_s \cos\frac{\phi}{2} - z_s \sin\frac{\phi}{2}, \qquad x_o = x_s \cos\frac{\phi}{2} + z_s \sin\frac{\phi}{2},$$

$$y_i = y_s, \qquad (3a) \qquad y_o = y_s, \qquad (3b)$$

$$z_i = z_s \cos\frac{\phi}{2} + x_s \sin\frac{\phi}{2} + l_i, \qquad z_o = z_s \cos\frac{\phi}{2} - x_s \sin\frac{\phi}{2} + l_o.$$

We consider incoming radiation of given curvature and of arbitrary amplitude profile $A^i(r_i)$, consisting of various modes (m,n) with the same $R_i(z)$. If both incident and reflected radiation are expanded into eigenmodes,

$$A^i(r_i) = e^{i\Phi_i(r_i)} \sum_{m,n} c^i_{mn} \frac{u_{mn}(r_i)}{\left[1 + \frac{z_i^2}{b_i^2}\right]^{1/2}} e^{i\delta_{mn}}, \qquad (4a)$$

$$A^o(r_o) = e^{i\Phi_o(r_o)} \sum_{p,q} c^o_{pq} \frac{u_{pq}(r_o)}{\left[1 + \frac{z_o^2}{b_o^2}\right]^{1/2}} e^{i\delta_{pq}}, \qquad (4b)$$

where

$$\Phi_i(r) = k\left[z + \frac{x^2 + y^2}{2R_i(z)}\right], \qquad (4c)$$

the relation among the incident and reflected expansion coefficients c^{i}_{mn}, c^{o}_{pq} is formulated by

$$c^{o} = \mathbf{R}\, c^{i}, \tag{5a}$$

or

$$c^{o}_{pq} = \sum_{m,n} R^{mn}_{pq}\, c^{i}_{mn}, \tag{5b}$$

where R^{mn}_{pq} are the elements of the reflection matrix **R**.

We examine the case when the mirror dimensions ρ are much larger than the wavelength λ, $\lambda << \rho$ (otherwise diffraction rather than reflection would prevail). We also assume that the angle ζ subtended by the mirror $\zeta = \rho/R_m$, where R_m parametrizes the radius of curvature, is small, of the order of the diffraction angle θ_d, $\zeta \sim \theta_d \sim \varepsilon$. The ν-th component of the reflected vector potential at distance $|\mathbf{r}_o - \underline{r}_o| >> \lambda$ from the mirror surface S is then given by

$$A^{o}_{(\nu)}(\mathbf{r}_o) = -\frac{ik}{2\pi} \iint_S ds\, \frac{e^{ik|\mathbf{r}_o - \underline{r}_o|}}{|\mathbf{r}_o - \underline{r}_o|} A^{S}_{(\nu)}(\underline{r}_o)\, (\hat{n} \cdot \hat{\delta r}). \tag{6}$$

In Eq. (6) $\hat{n}\cdot\hat{\delta r}$ is the obliqueness factor where $\hat{\delta r} = (\mathbf{r}_o - \underline{r}_o)/|\mathbf{r}_o - \underline{r}_o|$ and $\hat{n}$ is the normal unit vector to the reflecting surface. The surface element ds is given by $ds = \delta[z_o - f(x_o, y_o)]dx_o dy_o dz_o$ where $z_o = f(x_o, y_o)$ is the surface equation. Equation (6) is the convolution of a source term $A^{S}(\underline{r}_o)$ at the mirror surface with the propagator $\exp(ik|\mathbf{r}_o - \underline{r}_o|)/|\mathbf{r}_o - \underline{r}_o|$, i.e., a superposition of spherical waves originating at S. The source term $A^{S}(\underline{r}_o)$ is specified from the incoming vector potential $A^{i}(\underline{r}_i)$ through the boundary conditions and the coordinate transformations (3). We will assume a perfectly conducting surface, where the incident and reflected fields are related by

$$A^s = -A^i + 2\,(\hat{n}\cdot A^i)\,\hat{n}, \tag{7a}$$

and $\hat{n}$ is the normal unit vector to the reflecting surface. The second term in (7a) introduces a coupling among different vector components, caused by the mirror curvature. This cross-coupling is small and disappears in the plane mirror limit,

$$A^s_{(\nu)} = -A^i_{(\nu)}, \tag{7b}$$

where A^i and A^s are expressed in the incoming and outgoing coordinate systems respectively. Because of the linear superposition principle, Eq. (6), the cross-coupling contribution can be added separately, and will be deferred until Sec. VII. In the next three sections we will treat the reflected vector components as independent scalars, according to (7b), that corresponds to a phase shift by π during reflection. Most of the computations will be performed on the mirror surface. To simplify the notation from now on, we drop the bar (_) under the mirror coordinates $\underline{r}$. Subscripted quantities such as r_i, r_o, r_s will signify the mirror coordinates in each reference frame. Unsubscripted coordinates will denote the observation point in the reflected radiation frame of reference.

We seek cases when the reflected radiation propagates along z_o, contained within a cross section of dimensions $x,y \ll z-z_o$. The expansion $|r-r_o| \simeq (z-z_o)\,\{1 + [(x-x_o)^2 + (y-y_o)^2]/2(z-z_o)^2\}$ replaces the full propagator inside (6) with the paraxial propagator in that direction,

$$A^o(r) = \iint_S ds\; A(r_o)\,(\hat{n}\cdot\delta\hat{r})\,U_{-k}(r,r_o), \tag{8a}$$

where

$$U_{-k}(\mathbf{r}, \mathbf{r}_o) = \frac{ik}{2\pi} \frac{e^{-ik(z-z_o)}}{z-z_o} e^{-ik \frac{(x-x_o)^2 + (y-y_o)^2}{2(z-z_o)}} . \qquad (8b)$$

Expression (8) is the approximation of the exact solution (6) to order $[(x-x_o)^2 + (y-y_o)^2]/2(z-z_o)^2 \sim \varepsilon^2$. It is valid provided the surface S produces focused reflection along the desired direction. Otherwise the paraxial limit will fail to encompass all the radiation contained in the original expression (6). The geometry of the mirror that is compatible with the above approximation will be obtained during the computation of the reflection matrix.

It is known that the profile of a given eigenmode $A_{mn}(x_o,y_o,z_o)$ at z_o is generated by the propagator $U_k(\mathbf{r},\mathbf{r}_o)$ acting on the mode $A_{mn}(x,y,0)$ at z = 0. The inverse propagator $U_{-k}(\mathbf{r},\mathbf{r}_o)$ therefore reproduces $A_{mn}(x,y,0)$ from $A_{mn}(x_o,y_o,z_o)$,

$$\iint_S dx_o dy_o \frac{u_{mn}(x_o,y_o,z_o)}{\left[1 + \frac{z_o^2}{b_o^2}\right]^{1/2}} e^{-ik\left[z_o + \frac{x_o^2 + y_o^2}{2R(z_o)}\right]} U_{-k}(r,r_o) = u_{mn}(x,y,0). \quad (9)$$

This suggests multiplying and dividing the integrand inside (8a) by $\exp[i\Phi(\mathbf{r}_o)] / [1 + z_o^2/b_o^2]^{1/2}$, recasting (8a) in the form,

$$A^o(\mathbf{r}) = \iint ds\, e^{i\Delta(\mathbf{r}_o)} S(\mathbf{r}_o)\, e^{-i\Phi_o(\mathbf{r}_o)}\, U_{-k}(\mathbf{r},\mathbf{r}_o), \qquad (10)$$

where the source term $S(\mathbf{r}_o)$ is,

$$S(\mathbf{r}_o) = A^i[\mathbf{r}_i(\mathbf{r}_o)]\, (\hat{n} \cdot \delta\hat{r}) \left[1 + \frac{z_o^2(\mathbf{r}_o)}{b_o^2}\right]^{1/2}, \qquad (11)$$

and the phase term $\Delta(\mathbf{r}_o) = \Phi_i[\mathbf{r}_i(\mathbf{r}_o)] + \Phi_o(\mathbf{r}_o)$ is given by,

$$\Delta(\mathbf{r}_o) = k\left[z_i(\mathbf{r}_o) + z_o + \frac{x_i^2(\mathbf{r}_o) + y_i^2(\mathbf{r}_o)}{2R_i(\mathbf{r}_o)} + \frac{x_o^2 + y_o^2}{2R_o(\mathbf{r}_o)}\right]. \quad (12)$$

The phase $\Delta(\mathbf{r}_o)$ depends on the angle ϕ through the coordinate transformations Eqs. (3).

The term $\exp[i\Delta(\mathbf{r}_o)]$ is varying rapidly, on the scale of the wavelength λ. Therefore, its convolution with the slowly varying source term over an arbitrary surface will be vanishingly small. In general, this corresponds to radiation scattering where only a small fraction of the incoming radiation is reflected along the considered direction ϕ. The integral (10) will be finite only when it is possible to satisfy the condition $\Delta(\mathbf{r}_o) \simeq$ constant over some surface S. If, in addition, S is much larger than λ, expression (10) will be finite only within a narrow angle $\delta\phi$ around ϕ. This guarantees that the reflected radiation remains focused along that direction. Therefore, a condition that the exact reflected radiation (6) be fully covered by the paraxial limit (10) is that

$$\Delta(\mathbf{r}_o) = \text{constant}, \quad (13)$$

along the surface S. Accordingly, the optical path is the same along the rays connecting an incoming wave front with its mirror image (reflected) wave front.

Requirement (13) defines the appropriate mirror surface $z_o = f_o(x_o, y_o; \phi)$ for reflection in the elected direction. Assuming that f_o is found, we may express z_o in terms of x_o, y_o and use the constancy of $\Delta(\mathbf{r}_o)$ over S, reducing (10) into

$$A^o(\mathbf{r}) = \iint_S dx_o dy_o\ \sigma(x_o, y_o)\ e^{-i\Phi_o(x_o, y_o)}\ U_{-k}(\mathbf{r}, \mathbf{r}_o). \quad (14)$$

$\sigma(x_o,y_o) \equiv S[x_o,y_o,z_o(x_o,y_o)]$ is fully expanded in terms of $u_{mn}(x_o,y_o)$ that form a complete set in two dimensions,

$$\sigma(x_o,y_o) = \sum_{m,n} R^{mn}\, u_{mn}(x_o,y_o;W_o). \tag{15}$$

The expansion coefficients R^{mn} for Gaussian incoming radiation of arbitrary profile $\sigma(x_o,y_o)$ are given by

$$R^{mn} = \iint dx_o dy_o\ \sigma(x_o,y_o)\ u_{mn}(x_o,y_o;W_o) / \iint dx_o dy_o u_{mn}^{\,2}(x_o,y_o;W_o). \tag{16}$$

The radiation spot size W_o at the location of the mirror center is a free parameter, yet to be specified. Each choice of W_o generates an equivalent representation for $\sigma(x_o,y_o)$.

Upon substituting expansion (15) inside the integral (14) and using the property (9) for the inverse propagator U_{-k}, the reflected vector potential assumes the final form

$$A^o(x,y,0) = \sum_{m,n} R^{mn}\, u_{mn}(x,y;W_o), \tag{17}$$

where $W_o(z) = w_o\,(1 + z^2/b_o^{\,2})^{1/2}$, $w_o = (2b_o/k)^{1/2}$. Expression (17) is a complete decomposition of the reflected radiation into paraxial eigenmodes for incident radiation of arbitrary profile. Therefore, condition (13) that defines the mirror surface is sufficient for the full reflection of paraxial (Gaussian) incoming light beams into paraxial beams only. The fraction of the electromagnetic flux incident on the mirror is conserved after reflection. If, on the other hand, (13) is seriously violated, the paraxial modes are inadequate to include all reflected radiation, and the incident flux is not conserved by expressions similar to (17).

III. MIRROR SURFACE.

To obtain the equation for S we express all quantities inside (12) in the mirror coordinate frame applying the transformations (3a) and (3b). Using the scaling $x_s/R_m \sim y_s/R_m \sim \varepsilon << 1$, $z_s/R_m \sim \varepsilon^2$ we obtain from (13)

$$z_s = -\frac{1}{2R_m \cos\frac{\phi}{2}}\left[x_s^2 \cos^2\frac{\phi}{2} + y_s^2\right], \tag{18a}$$

where

$$\frac{1}{R_m} = \frac{1}{2R_o} + \frac{1}{2R_i}. \tag{18b}$$

Equation (18a) is the analytic expression for a paraboloid surface. R_m parametrizes the mirror curvature, being positive or negative for a convex or concave mirror respectively. The surface is reflection symmetric with $(zx)_s$ and $(zy)_s$ as the symmetry planes; there is no rotational symmetry around $\hat{z}_s$. Surface (18a) can also be approximated, to second order in $(x_s/R_m)^2$, $(y_s/R_m)^2$ by hyperboloids or ellipsoids defined by

$$\left(z_s - R_m\cos\frac{\phi}{2}\right)^2 - x_s^2\cos^2\frac{\phi}{2} - y_s^2 = R_m^2\cos^2\frac{\phi}{2}, \tag{19a}$$

$$\left(z_s + R_m\cos\frac{\phi}{2}\right)^2 + x_s^2\cos^2\frac{\phi}{2} + y_s^2 = R_m^2\cos^2\frac{\phi}{2}. \tag{19b}$$

All the surfaces become spherical in the limit of perpendicular incidence $\phi = 0$, and plane mirrors when $R_m \to \infty$. Using the definition of the curvature for the paraxial modes, Eq. (2), and the fact that $R >> b$ in cases of interest, we obtain from (18b)

$$\frac{1}{R_o} = \frac{2}{R_m} - \frac{1}{R_i}. \tag{20}$$

Relation (20) defines the curvature of the reflected modes from the incoming mode curvature and the curvature of the mirror.

Equations (18)-(20) imply that

$$\Delta(r_s) \equiv \Delta[r_i(r_s), r_o(r_s)] = \text{const.} + O\left[k\rho \left(\frac{\rho}{R_m}\right)^2 \right], \qquad (21)$$

where ρ parametrizes the mirror size. A more complicated surface equation (higher than quadratic in x, y, z) is required to improve the constancy to a higher order. In the next section the reflection matrix will be computed by expansion in powers of $W_o/R_m \simeq \rho/R_m$. Since $k\rho >> 1$, the approximation $\Delta(r_s) = \text{constant}$ is satisfactory for a first order expansion as long as $\rho/R_m \sim 1/k\rho$. In case that $\rho/R_m > 1/k\rho$, $\Delta(x_s, y_s)$ is a slowly varying function over S. Large mirrors require the inclusion of the phase slippage term $\exp[i\Delta(x_s, y_s)]$ next to the source term $\sigma(x_s, y_s)$ in Eq. (16).

The unit vector $\hat{n}$ normal to the mirror surface is given by

$$\hat{n} = \frac{\nabla f}{|\nabla f|} \simeq \cos\frac{\phi}{2}\,\frac{x_s}{R_m}\,\hat{x}_s + \frac{1}{\cos\frac{\phi}{2}}\,\frac{y_s}{R_m}\,\hat{y}_s + \left(1 + \frac{z_s}{R_m \cos\frac{\phi}{2}}\right)\hat{z}_s,$$

where $f(x_s, y_s, z_s)$ is given by Eq. (18a).

IV. COMPUTATION OF THE REFLECTION MATRIX

According to the definition (5b), the R_{pq}^{mn} element of the reflection matrix **R** is obtained from the source term $\sigma_{pq}(x_o,y_o)$ inside (14) generated by a single incident eigenmode $A_{pq}[r_i(r_o)]$. The integration is performed in the mirror-aligned coordinates, taking advantage of the existing symmetries. The coordinates r_i and r_o, defining the incoming and outgoing wave functions, become explicit functions of x_s, y_s through the transformations (3). The surface equation (14a) is used to express z_s in terms of (x_s,y_s). The mirror boundary

$$x_s^2\cos^2\frac{\phi}{2} + y_s^2 = \rho^2 \tag{22}$$

is defined by the intersection of the infinite surface (18a) with the plane $z_s = \text{const} = 2\rho^2\cos^2(\phi/2)/R_m$. After the above manipulations, the reflection matrix elements take the form

$$R_{pq}^{mn} = \iint_S dx_s dy_s \frac{\bar{u}_{mn}(x_s,y_s)\bar{u}_{pq}(x_s,y_s)}{\left[1 + \frac{l_o^2}{b_o^2}\right]^{1/2}} \left[\frac{1 + \frac{z_o^2(x_s,y_s)}{b_o^2}}{1 + \frac{z_i^2(x_s,y_s)}{b_i^2}}\right]^{1/2} e^{i\Delta(x_s,y_s)}$$

$$\times e^{i\delta_{pq}^i(x_s,y_s) - i\delta_{mn}^o(x_s,y_s)} \left[\cos\frac{\phi}{2}\left(1 - \frac{x_s}{R_m}\sin\frac{\phi}{2} - \frac{x_s^2\sin^2\frac{\phi}{2}}{R_m^2}\right)\right], \tag{23}$$

where

$$\bar{u}_{mn}(x_s,y_s) \equiv u_{mn}\left[x_o(x_s,y_s),\ y_s\right],\ \bar{u}_{pq}(x_s,y_s) \equiv u_{pq}\left[x_i(x_s,y_s),\ y_s\right]. \tag{24}$$

Expression (23) is correct to order ρ^2/R_m^2.

It will be seen that **R**, as given by (23), depends on four parameters

$$\mathbf{R} \equiv \mathbf{R}(\phi,\ \alpha,\ \mu;\ \xi). \tag{25}$$

ϕ is the reflection angle shown in Fig. 2. α is the ratio of the incoming to the outgoing spot size at the mirror, $\alpha = W_i(l_i)/W_o(l_o)$. $\mu = \rho/W_o$ parametrizes the mirror size compared to the radiation spot size. $\xi = W_o/R_m$ scales as the diffraction angle $\theta_d \simeq W_o/l_o$ multiplied by the curvature mismatch R_o/R_m between the mirror and the radiation wavefronts. The spot size W_o enters as a free parameter because only the curvature $1/R_o$ for the reflected modes is specified by the mirror geometry. Since many combinations of W_o and l_o apply to a given curvature according to paragraph Eq. (2), an additional selection rule for W_o is needed. Note that W_o does not have to match W_i. This is obvious in cases when the mirror size ρ is smaller that W_i. Each value of W_o defines a complete set of modes for the reflected radiation and an equivalent representation for **R**.

Parameters ϕ, α, and μ can be arbitrary. In most cases of interest, however, ξ is small, $\xi \ll 1$, of the same order as the diffraction angle θ_d. The analytic computation of the matrix elements is carried out by expanding the integral (23) in powers of ξ,

$$\mathbf{R} = \mathbf{R}(0) + \xi\, \mathbf{R}(1) + \xi^2\, \mathbf{R}(2). \tag{26}$$

Each representation of **R** is tied to the choice of the basis functions $u_{mn}(\mathbf{r})$. The eigenmodes $u_{mn}(\mathbf{r})$ are specified according to the coordinate geometry. In the next subsections we derive **R** in Gaussian-Hermite and Gaussian-Laguerre representations. For simplicity, it is assumed that $\Delta(x_s,y_s)$ in Eq. (23) is constant, i.e., $k\rho\ (\rho/R_m) \ll 1$.

(a). Gaussian-Hermite representation

In rectangular coordinates (x,y,z) the functions $u_{mn}(x,z;W)$ are given by

$$u_{mn}(x,y;W) = a_{mn} H_m\left(\frac{\sqrt{2}x}{W}\right) H_n\left(\frac{\sqrt{2}y}{W}\right) e^{-\frac{x^2+y^2}{W^2}}, \tag{27a}$$

where H_m, H_n are the Hermite polynomials and a_{mn} is a normalization factor, setting the total electromagnetic flux carried by the mode equal to unity,

$$a_{mn} = \frac{\sqrt{2}}{W}\left(\pi\, 2^{m+n}\, m!n!\right)^{-1/2}. \tag{27b}$$

The corresponding slow phase factor $\delta_{mn}(z)$ in Eq. (2) is

$$\delta_{mn}(z) = (m + n + 1)\, \tan^{-1}\left(\frac{z}{b}\right). \tag{27c}$$

Substituting inside (23), expanding in ξ and performing the integrations, Eqs. (23)-(26) yield

$$R^{mn}_{pq}(0) = C^{mn}_{pq}\, e^{i\psi^{mn}_{pq}}\, I^{mn}_{pq}, \tag{28a}$$

$$R^{mn}_{pq}(1) = C^{mn}_{pq}\, e^{i\psi^{mn}_{pq}}\, \tan\frac{\phi}{2}\left\{M^{mn}_{pq} + i\, N^{mn}_{pq}\right\}, \tag{28b}$$

where C^{mn}_{pq} is a normalization factor

$$C^{mn}_{pq} = \frac{W_o}{\pi W_i}\left(2^{m+n+p+q}\, m!n!p!q!\right)^{-1/2}, \tag{28c}$$

and the phase ψ^{mn}_{pq} is expressed by

$$\psi^{mn}_{pq} = (p+q+1)\tan^{-1}\left(\frac{l_i}{b_i}\right) - (m+n+1)\tan^{-1}\left(\frac{l_o}{b_o}\right) + k(l_i+l_o). \tag{28d}$$

$$I_{pq}^{mn} = \int_{-X_s}^{X_s} dX \int_{-Y_s}^{Y_s} dY \; H_p(\alpha X)\, H_q(Y)\, H_m(X)\, H_n(Y)\, e^{-\frac{\alpha^2+1}{2}(X^2+Y^2)}, \quad (29a)$$

$$M_{pq}^{mn} = \int_{-X_s}^{X_s} dX \int_{-Y_s}^{Y_s} dY \; H_p(\alpha X)\, H_q(Y)\, H_m(X)\, H_n(Y)\, e^{-\frac{\alpha^2+1}{2}(X^2+Y^2)}$$

$$\left\{ -\frac{3}{2} X + \frac{1-\alpha^2}{\sqrt{2}} X(X^2+Y^2) - \left(\alpha \frac{H_p'(\alpha X)}{H_p(\alpha X)} - \frac{H_m'(X)}{H_m(X)} \right) \frac{\sqrt{2}}{4} (X^2+Y^2) \right\}, \quad (29b)$$

$$N_{pq}^{mn} = \int_{-X_s}^{X_s} dX \int_{-Y_s}^{Y_s} dY \frac{X}{\sqrt{2}} \; H_p(\alpha X)\, H_q(Y)\, H_m(X)\, H_n(Y)\, e^{-\frac{\alpha^2+1}{2}(X^2+Y^2)}. \quad (29c)$$

In the rescaled variables $X \simeq \cos\phi/2 \; \sqrt{2}x_s/W_o$, $Y = \sqrt{2}y_s/W_o$, the surface boundary is given by $X_s^2 + Y_s^2 = 2\rho^2/W_o^2$. The lowest terms can be computed directly. The matrix elements are computed, to first order in ξ, in Appendix A for large size mirror and $\alpha = 1$.

(b). Gaussian-Laguerre representation

In cylindrical coordinates (r,θ,z) where $\tan\theta = x/y$, $r = (x^2+y^2)^{1/2}$, $u_m^p(r,\theta;W)$ take the form

$$u_m^{\pm p}(r,\theta;W) = a_m^p \begin{pmatrix} \cos p\theta \\ \sin p\theta \end{pmatrix} \left(\frac{\sqrt{2}r}{W}\right)^p L_m^p\left(\frac{2r^2}{W^2}\right) e^{-\frac{1}{2}\frac{2r^2}{W^2}}, \quad (30a)$$

where +p(-p) signifies cosine (sine) poloidal dependence, a_m^p is given by

$$a_m^p = \left(\frac{4}{\pi W^2}\right)^{1/2} \left(\frac{m!}{(m+p)!}\right)^{1/2}, \quad (30b)$$

and the L_m^p are the Laguerre polynomials. The corresponding slow phase $\delta_m^p(z)$ in Eq. (2) is,

$$\delta_m^p(z) = (2m + p + 1) \tan^{-1}\left(\frac{z}{b}\right). \tag{30c}$$

The transformations among polar coordinates representing the various reference frames are

$$r_i \simeq r_s \left[1 - \sin^2\theta_s \sin^2\frac{\phi}{2} - 2\frac{z_s}{R_m}\sin\theta_s \sin\frac{\phi}{2}\cos\frac{\phi}{2}\right]^{1/2},$$

$$r_o = r_s \left[1 - \sin^2\theta_s \sin^2\frac{\phi}{2} + 2\frac{z_s}{R_m}\sin\theta_s \sin\frac{\phi}{2}\cos\frac{\phi}{2}\right]^{1/2}, \tag{31a}$$

$$\tan\theta_i = \cos\frac{\phi}{2}\tan\theta_s - \frac{z_s}{r_s}\frac{\sin\frac{\phi}{2}}{\cos\theta_s},$$

$$\tan\theta_o = \cos\frac{\phi}{2}\tan\theta_s + \frac{z_s}{r_s}\frac{\sin\frac{\phi}{2}}{\cos\theta_s}. \tag{31b}$$

The mirror surface (18a) is expressed in polar coordinates as

$$z_s = -\frac{r_s^2}{2R_m}\frac{\sin^2\theta_s\cos^2\frac{\phi}{2} + \cos^2\theta_s}{\cos\frac{\phi}{2}}. \tag{31c}$$

Applying similar computational procedure as in the previous subsection we obtain

$$R_{mn}^{pq} = C_{mn}^{pq}\, e^{i\psi^{pq}} \cos\frac{\phi}{2}\int_0^{X_s} dX \left\{D^{pq}(X)U^{pq}(X) + \xi \sin\frac{\phi}{2} E^{pq}(X)\left[V_{mn}^{pq}(X) + i\, W_{mn}^{pq}\right]\right\}, \tag{32a}$$

$$C_{mn}^{pq} = \frac{1}{2\pi}\left[\frac{m!n!\ \alpha^2}{(m+p)!(n+q)!}\right]^{1/2} , \tag{32b}$$

and the phase ψ_{mn}^{pq} is expressed by

$$\psi_{mn}^{pq} = (2m+p+1)\ \tan^{-1}\left(\frac{l_i}{b_i}\right) - (2n+q+1)\ \tan^{-1}\left(\frac{l_o}{b_o}\right) + k(l_i+l_o) . \tag{32c}$$

The integrals D^{pq}, E^{pq}, U_{mn}^{pq}, V_{mn}^{pq} and W_{mn}^{pq} are given by

$$D^{pq}(X) = \int_o^{2\pi} d\theta_m \frac{\cos p\left[\theta_i(\theta_s)\right] \cos q\left[\theta_o(\theta_s)\right]}{1 - \sin^2\frac{\phi}{2}\sin^2\theta_m} , \tag{33a}$$

$$E^{pq}(X) = \int_o^{2\pi} d\theta_m \frac{\sin\theta_m \cos p\left[\theta_i(\theta_s)\right] \cos q\left[\theta_o(\theta_s)\right]}{(1 - \sin^2\frac{\phi}{2}\sin^2\theta_m)^{3/2}} , \tag{33b}$$

$$U_{mn}^{pq}(X) = (\alpha^2 X)^{\frac{p}{2}}\ X^{\frac{q}{2}}\ L_m^p(\alpha^2 X)\ L_n^q(X)\ e^{-\frac{\alpha^2+1}{2}X} , \tag{33c}$$

$$V_{mn}^{pq}(X) = \frac{1}{\sqrt{2}}\left\{\frac{p-q}{2} - 3 - \frac{\alpha^2+1}{2}X + \left[\frac{L_m^{p\prime}(\alpha^2 X)}{L_m^p(\alpha^2 X)} - \frac{L_n^{q\prime}(X)}{L_n^q(X)}\right]X\right\}$$

$$(\alpha^2 X)^{\frac{p}{2}}\ X^{\frac{q+1}{2}}\ L_m^p(\alpha^2 X)\ L_n^q(X)\ e^{-\frac{\alpha^2+1}{2}X} , \tag{33d}$$

$$W_{mn}^{pq}(X) = \frac{1}{\sqrt{2}}\ (\alpha^2 X)^{\frac{p}{2}}\ X^{\frac{q+1}{2}}\ L_m^p(\alpha^2 X)\ L_n^q(X)\ e^{-\frac{\alpha^2+1}{2}X} . \tag{33e}$$

In obtaining (33a) - (33e), X was defined by $X = [1-\sin^2(\phi/2)\sin^2\theta]r^2/2W_o^2$; thus, according to (22) and (30), the boundary X_s is $X_s = 2\rho^2/W_o^2$. The lowest order terms for the first few elements are given in Appendix B for arbitrary deflection angle ϕ and $\alpha = 1$.

V. LIMITING CASES

When the mirror radius tends to infinity ($1/R_m \to 0$), or in cases of vertical incidence on the mirror ($\phi = 0$), the higher order corrections in the reflection matrix **R** disappear,

$$\mathbf{R} = \mathbf{R}(0) \tag{34}$$

in both representations. The nondiagonal elements in **R** stem from the finite mirror size only. If, in addition, the mirror size is very large, $\mu \gg 1$, it is appropriate to take $W_o = W_i$ as best representation for the reflected radiation. The $\alpha = 1$ limit yields

$$R^{mn}_{pq} = \delta^{mn}_{pq}. \tag{35}$$

Thus, in case of large curved mirror and vertical incidence, or large plane mirror and arbitrary incidence, the reflection matrix is the identity matrix.

The case $\alpha = 1$ is of special interest for arbitrary angle of deflection ϕ and mirror curvature $1/R$, as it will be explained in the next section. For finite mirror size $\rho \geq W_o$, ($\mu \geq 1$), there exists zeroth order non-diagonal terms inside **R**(0). Since **R**(0) is independent of the angle of deflection ϕ, the finite mirror size yields the dominant contribution to the reflection into modes different than the incoming. The effects of the deflection of the light beam enter to first order in ξ, **R**(1), or higher. In the Hermite representation the elements $R^{mn}_{pq}(0)$ couple mode combinations with $m + p$ = even, $n + q$ = even. The elements with either $m + p$ or $n + q$ odd vanish because of the even/odd symmetry of the Hermite functions.

As the mirror size becomes very large and the limits of integration in (23) are extended, the orthogonality among the various modes $u_{mn}(\mathbf{r}_s)$ becomes effective. The off-diagonal terms in **R**(0) become comparable to

the first order corrections roughly when $1/\mu^2 \sim \xi \sim \theta_d$. At the limit $\mu \to \infty$ all the nondiagonal elements of **R** are reduced to order ξ or higher,

$$R^{mn}_{pq} = \xi\, R^{mn}_{pq}(1) + O(\xi^2), \quad m \neq p,\ n \neq q, \tag{36a}$$

and the only matrix elements of zeroth order in ξ are the diagonal

$$R^{mn}_{mn} = R^{mn}_{mn}(0) + O(\xi^2), \tag{36b}$$

in both Hermite and Laguerre represenations. The lowest correction in the diagonal elements is of second order ξ^2, while the first order contribution disappears. This is consistent with flux conservation during reflection in case of large mirror.

In obtaining Eqs. (28) and (32) it was assumed that $\Delta(x_s, y_s)$ is constant over S. According to (21) the variation of Δ is parametrized by $\xi^* = (kW_i^2/R_m)\,\xi$. When $(kW_i^2/R_m) \geq 1$, ξ^* becomes of order ξ and the effects of the slow phase slippage must be retained in (23). This effect, known as spherical aberration, causes additional corrections $\mathbf{R}^*(1)$, of order ξ^*,

$$\mathbf{R} = \mathbf{R}(0) + \xi\,\mathbf{R}(1) + \xi\,\overset{*}{\mathbf{R}}(\overset{*}{1}) + \ldots\ldots$$

Spherical aberration does not disappear at the limit of large mirror size, as opposed to the effects discussed so far. In fact, when $\xi^* > \xi$, it places a lower limit on the off-diagonal terms in the reflection matrix,

$$R^{mn}_{pq} \geq \xi^*\, R^{mn}_{pq}(1)^*.$$

Perfect reflection, requiring $\xi^* = 0$, is possible only for plane mirror ($R_m \to \infty$) of large size.

The superposition principle can be used to describe reflection from more complex mirror surfaces. In case of a mirror with a hole the surface integral (14) over S_m is expressed as $\int_S = \int_{S1} - \int_{S2}$ where S_1 is defined by the mirror exterior boundary and S_2 is the surface of the hole. The total

reflection matrix **R** is given by $\mathbf{R} = \mathbf{R}(S_1) - \mathbf{R}(S_2)$, the difference in the reflection matrices associated with mirrors S_1 and S_2 respectively. The transmission matrix **T** through a screen with an aperture of area S is given by $\mathbf{T} = -\mathbf{R}$, **R** being the reflection matrix for a mirror matching the aperture S. The transmission matrix for radiation diffracted behind a finite size mirror is given by $\mathbf{T}' = 1 - e^{i\pi}\mathbf{R}$ where 1 is the identity matrix.

VI. REFLECTION OF THE LOWEST ORDER MODE

The computation of all the truncated integrals for finite mirror surface is nontrivial. Most applications, however, involve the (0,0) lowest order mode as the dominant mode in both incoming and reflected radiation. The strategy here is to compute the element R_{00}^{00} of the reflection matrix first. Then the waist for the reflected modes W_o can be selected so that it maximizes R_{00}^{00}. The optimum representation condition

$$\frac{\partial R_{00}^{00}}{\partial \alpha} = 0, \tag{37}$$

puts the maximum amount of the reflected radiation in the lowest order mode (a different mode and matrix element may be chosen, if desired). It is pointed out that (37) does not improve the properties of the reflected radiation. It enables one to choose the best representation in terms of minimizing the coefficients of the undesired modes for the scattered radiation. Once W_o is fixed by (37) then the exact location and size of the waist(s) for the reflected modes is determined by solving the system of equations

$$\frac{1}{R_o} = \frac{l_o}{l_o^2 + b_o^2}, \tag{38a}$$

$$W_o = w_o \left[1 + \frac{l_o^2}{b_o^2}\right]^{1/2}. \tag{38b}$$

The element R_{00}^{00} is identical in both representations since the lowest order mode u_{00} is the same in rectangular and cylindrical coordinates. Performing the integration (29a) yields R_{00}^{00} to first order in ξ

$$R_{00}^{00} = \frac{2\alpha}{1+\alpha^2}\left[1 - e^{-(1+\alpha^2)\mu^2}\right] + O(\xi^2). \qquad (39)$$

Note that the first order term vanishes and the lowest correction is of second order in ξ^2. The exact dependence on the mirror size ρ is parametrized by $\mu = \rho/W_o$, while $\alpha = W_i/W_o$ parametrizes the ratio of the incoming and scattered radiation spot sizes at the mirror. The optimization condition $\partial R_{00}^{00}(0)/\partial\alpha = 0$ yields, $\alpha^2 = 1 + \exp[-(1+\alpha^2)\mu^2][2\mu^2\alpha^4+(2\mu^2+1)\alpha^2-1]$. In case that the mirror cross section is much larger than the spot size of the incoming mode, $\mu >> 1$, $\alpha \rightarrow 1$ and the reflected spot size at the mirror matches the incoming, $W_o = W_i$.

Large mirror size is desired to maximize the total reflection coefficient. For incoming radiation of unity electromagnetic flux $P_i = |c^i|^2 = \Sigma\ |c^i{}_{pq}|^2 = 1$, the total reflection coefficient $\eta_R = P_o/P_i$ equals the reflected flux P_o,

$$P_o = |c^o|^2 = |\ R \cdot c^i|^2 = \sum_{mn}\sum_{pq} |R_{pq}^{mn}\ c^i{}_{pq}|^2. \qquad (40)$$

In Fig. 3 we plot η_R for the lowest order incoming mode as a function of $\mu' = \cos(\phi/2)\ \rho/W_o = \cos(\phi/2)\ \mu$. μ' parametrizes the size of the mirror projection into the plane perpendicular to the incoming radiation direction. The incoming radiation has a wavelength $\lambda = 1\mu$ (10^{-4}cm), waist $w_i = 2\times10^{-1}$cm at distance $l_i = 1.8\times10^{2}$cm from the mirror and radius of curvature (at the mirror) $R_i = 8.95\times10^{3}$cm. The mirror has a radius of curvature $R_m = 8.95\times10^{3}$cm, yielding reflected modes of $R_o = 8.95\times10^{3}$ (again l_o and w_o depend on the choice of W_o). In Fig. 4 we plot the magnitude of the reflection coefficients $|R_{pq}^{00}|$ of the lowest order mode (0,0) into the firstr 25 modes (p,q) with $p \leq q \leq 5$, as a function of μ'. The deflection angle is 90^o and the ratio of the spot

sizes is 1. Increasing mirror size maximizes the diagonal element and minimizes scattering into other modes. The spherical aberration was retained inside (23) in evaluating the matrix elements. Its effect is small, since for the above parameters $\xi^* \approx 0.28\xi$, and a good agreement is observed with the constant Δ theoretical limit. In particular, the dominant off-diagonal terms couple the (0,0) incoming mode to the (1,0), (3,0) and (3,2) reflected modes only, according to the selection rules, Eqs. A(10). Comparing Figs. 3 and 4 with the next plots shows that the relative mirror size to the radiation spot size is the most important parameter to determine the reflection into other than the incoming modes.

In Fig. 5 we fix the mirror size $\mu' = 2$ and the angle $\phi = 90^o$ and vary the spot size ratio α. The best representation, maximizing R_{00}^{00} and minimizing R_{pq}^{00} is obtained at $\alpha = 1$. However, for small mirror $\mu' = 0.66$, the maximum for R_{00}^{00} occurs at $\alpha \approx 0.70$ (see Fig. 6). Radiation reflected off mirrors smaller than the incoming spot size is best described by outgoing modes of reduced spot size $W_o < W_i$. Also note from Fig. 6b that for small mirror size the total power reflected into the first 25 modes never exceeds 80% of the incoming flux; even with many more modes η_R remains less than 1. In Fig. 7 the reflection coefficients R_{pq}^{00} are plotted as functions of the angle of deflection ϕ for fixed $\alpha = 1$, $\mu' = 2$. It is seen that, for sufficiently large reflecting surface and good choice of the spot size W_o, the reflection matrix is not very sensitive to ϕ and the off-diagonal terms remain small.

The main conclusions so far are summarized as follows. When the mirror size is ≥ 2.5 times the incoming spot size, the fraction of the incident power scatterd into different modes is of order ξ^2 for

$kW^2_i/R_m < 1$, or $(\xi^*)^2$ for $kW^2_i/R_m > 1$. This holds for a wide range of deflection angles ϕ. It will be shown in the next section that cross-polarization effects are of the same order. In most applications both ξ and ξ^* are less than 10^{-2}. To this end, scattering losses will be smaller than the losses caused by the finite reflectivity (i.e., absorption) by the mirror, for most dielectrics.

VII. CROSS-POLARIZATION EFFECTS

The curvature of the mirror surface produces a cross-coupling between the transverse components of the incoming and reflected radiation. Inserting expressions (21) for the normal unit vector to the mirror inside the boundary conditions Eq. (7a), the full source term $\mathbf{A}^s = (A_x^s, A_y^s, A_z^s)$ for an incoming wave $\mathbf{A}^i = (A_x^i, A_y^i, 0)$ is given by

$$A_x^s = - A_x^i + 2 \tan\frac{\phi}{2} \frac{y_s}{R_m} A_y^i,$$

$$A_y^s = - A_y^i + 2 \tan\frac{\phi}{2} \frac{y_s}{R_m} A_x^i,$$

$$A_z^s = 2 \cos\frac{\phi}{2} \frac{x_s}{R_m} A_x^i + 2 \frac{y_s}{R_m} . \qquad (41)$$

In the above relations, the components of $\mathbf{A}^i$ and $\mathbf{A}^s$ are given in coordinate systems aligned with the incoming and outgoing radiation, respectively. According to (41) the reflection of a plane polarized wave generates components polarized in every direction, including A_z. These cross polarization effects enter to order ξ and result in a small rotation of the polarization angle.

The radiation steming from the A_z^s component will propagate perpendicularly to the direction of interest $\hat{z}_o$ and escapes the resonator as pure reflection loss. The relation between the incoming and reflected transverse components, including cross-polarization effects, is now given by

$$\begin{pmatrix} C_x^o \\ C_y^o \end{pmatrix} = \begin{pmatrix} R & Q \\ Q & R \end{pmatrix} \begin{pmatrix} C_x^i \\ C_y^i \end{pmatrix}. \qquad (42)$$

The matrix $\mathcal{R}$ has been computed in the previous section. Substitution

of the additional cross-terms in Eq. (41) inside the propagator integral (6) yields

$$Q_{(xy)pq}^{mn} = Q_{(yx)pq}^{mn} = Q_{pq}^{mn} ,$$

where

$$Q_{pq}^{mn} = \iint_S dx_s dy_s \; 2 \tan\frac{\phi}{2} \frac{y_s}{R_m} \frac{\bar{u}_{mn}(x_s,y_s)\bar{u}_{pq}(x_s,y_s)}{\left[1 + \frac{l_o^2}{b_o^2}\right]^{1/2}} \left[\frac{1 + \frac{z_o^2(x_s,y_s)}{b_o^2}}{1 + \frac{z_i^2(x_s,y_s)}{b_i^2}}\right]^{1/2}$$

$$\times \quad e^{i\delta_{pq}^{i}(x_s,y_s) - i\delta_{mn}^{o}(x_s,y_s)} \left[\cos\frac{\phi}{2}\left(1 - \frac{x_s}{R_m}\sin\frac{\phi}{2} - \frac{x_s^2 \sin^2\frac{\phi}{2}}{R_m^2}\right)\right] . \tag{43}$$

In Gaussian-Hermite representation, we obtain

$$Q_{pq}^{mn}(1) = \sqrt{2}\xi \, C_{pq}^{mn} \, e^{i\psi_{pq}^{mn}} \tan\frac{\phi}{2} \, G_{pq}^{mn} , \tag{44a}$$

with

$$G_{pq}^{mn} = \int_{-X_s}^{X_s} dX \int_{-Y_s}^{Y_s} dY \; H_p(\alpha X) \, H_q(Y) \, Y \, H_m(X) \, H_n(Y) \, e^{-\frac{\alpha^2+1}{2}(X^2+Y^2)} . \tag{44b}$$

In Gaussian-Laguerre representation, we have

$$Q_{mn}^{pq}(1) = \sqrt{2} \, \xi \sin\frac{\phi}{2} \int_0^{X_s} dX \; G_{mn}^{pq}(X) \, B^{pq}(X), \tag{45a}$$

where

$$G_{mn}^{pq}(X) = (\alpha^2 X)^{\frac{1}{2}} \, X^{\frac{q+1}{2}} \, L_m^p(\alpha^2 X) \, L_n^q(X) \, e^{-\frac{\alpha^2+1}{2} X} , \tag{45b}$$

and

$$B^{pq}(X) = \int_0^{2\pi} d\theta \; \frac{\cos\theta \cos\left[p\theta_i(\theta)\right]\cos\left[q\theta_i(\theta)\right]}{1 - \sin^2\frac{\phi}{2}\sin^2\theta} . \qquad (45c)$$

In both representations, cross polarization effects enter to order ξ. In case of vertical incidence ($\phi = 0$) with arbitrary curvature $1/R_m$, or plane mirror ($\xi \sim 1/R_m = 0$) and arbitrary incidence ϕ, $\mathbf{Q}$ goes to zero. Transverse vector components are reflected independently of each other in these two limits. Some of the elements of $\mathbf{Q}$ (in both representations) are given in Appendix C for large ($\rho >> W_i$) mirror.

Acknowledgment

This work was supported by SDIO and managed by SDC.

Appendix A. Computation of the Hermitian Matrix Elements.

The integrals (29) will be evaluated here in case the mirror size ρ is much larger than the incoming mode spot size W_i, $\rho \cos \phi/2 >> W_i$. Then the limits of the surface integrals can be extended to infinity, and the spot size for the outgoing modes W_o matches that of the incoming at the mirror, i.e., $\alpha = 1$. We use the notation

$$\psi_n = e^{-\frac{X^2}{2}} H_n(X), \tag{A1}$$

the recurrence relation

$$H_n'(X) = 2n\, H_{n-1}(X), \tag{A2}$$

and the orthonormality properties

$$\int_{-\infty}^{\infty} dX\, \psi_n(X)\psi_m(X) = 2^n n!\sqrt{\pi}\, \delta_{m,n}, \tag{A3}$$

$$\int_{-\infty}^{\infty} dX\, \psi_n(X)\, X\, \psi_m(X) \equiv \langle X \rangle_{m,n} = \sqrt{\pi}\left(2^{n-1} n!\, \delta_{m,n-1} + 2^n (n+1)!\, \delta_{m,n+1}\right), \tag{A4}$$

$$\int_{-\infty}^{\infty} dX\, \psi_n(X)\, X^2\, \psi_m(X) \equiv \langle X^2 \rangle_{m,n}$$

$$= \sqrt{\pi}\left\{2^{n-2} n!\, \delta_{m,n-2} + 2^{n-1}(2n+1) n!\, \delta_{m,n} + 2^n (n+2)!\, \delta_{m,n+2}\right\}, \tag{A5}$$

to obtain

$$I_{pq}^{mn} = \pi\, 2^{m+n} n!m!\, \delta_{p,m}\delta_{q,n}, \tag{A6}$$

$$M_{pq}^{mn} = -\frac{3}{2} \langle X \rangle_{p,m} \left(\sqrt{\pi}\, 2^n n!\right) \delta_{q,n},$$

$$- \frac{\sqrt{2}}{4}\left[2k\langle X^2\rangle_{p-1,m} - 2m\,\langle X^2\rangle_{m-1,p}\right]\left(\sqrt{\pi}\,2^n n!\right)\delta_{q,n}$$

$$- \frac{\sqrt{2}}{4}\left[2k\,2^m m!\;\delta_{p-1,m} - 2m\,2^{m-1}(m-1)!\,\delta_{p,m-1}\right]\langle Y^2\rangle_{q,n}, \quad \text{(A7)}$$

$$N_{pq}^{mn} = \frac{1}{\sqrt{2}}\left[(m+n+1)\frac{b_i R_m}{l_i R_i} + (p+q+1)\frac{b_o R_m}{l_o R_o}\right]\langle X\rangle_{p,m}\left(\sqrt{\pi}2^n n!\,\xi\right)\delta_{q,n}. \quad \text{(A8)}$$

Inserting expressions (A3)-(A5) into Eqs. (A6)-(A8) we obtain

$$R_{pq}^{mn}(0) = \delta_{p,m}\,\delta_{q,n}, \quad \text{(A9)}$$

$$R_{pq}^{mn}(1) = \quad \text{(A10)}$$

$$\tan\frac{\phi}{2}\left\{\left\{-\left[\frac{3}{2}\left(\frac{m-1}{2}\right)^{1/2} + \frac{1}{\sqrt{2}}\left(\frac{m-1}{2}\right)^{3/2} - \left(\frac{2m-1}{4} + \frac{2n+1}{4}\right)m^{1/2}\right]\delta_{p,m-1}\right.\right.$$

$$- \left[\frac{3}{2}\left(\frac{m+1}{2}\right)^{1/2} - \frac{1}{\sqrt{2}}\left(\frac{m+1}{2}\right)^{3/2} + \frac{1}{\sqrt{2}}\left(\frac{m+1}{2}\right)^{1/2}\left(\frac{2m+1}{2} + \frac{2n+1}{2}\right)\right]\delta_{p,m+1}$$

$$\left.\left. - \frac{1}{\sqrt{2}}\left(\frac{(m+1)(m+2)(m+3)}{8}\right)^{1/2}\delta_{p,m+3} + \frac{1}{\sqrt{2}}\left(\frac{m(m-1)(m-2)}{8}\right)^{1/2}\delta_{p,m-3}\right\}\delta_{q,n}\right.$$

$$- \frac{1}{\sqrt{2}}\left[\left(\frac{m+1}{2}\right)^{1/2}\delta_{p,m+1} - \left(\frac{m}{2}\right)^{1/2}\delta_{p,m-1}\right]\left(\frac{(n-1)(n-2)}{4}\right)^{1/2}\delta_{q,n-2}$$

$$- \frac{1}{\sqrt{2}}\left[\left(\frac{m+1}{2}\right)^{1/2}\delta_{p,m+1} - \left(\frac{m}{2}\right)^{1/2}\delta_{p,m-1}\right]\left(\frac{(n+1)(n+2)}{4}\right)^{1/2}\delta_{q,n+2}$$

$$+$$

$$\left.\frac{i}{\sqrt{2}}\left[(m+n+1)\frac{b_i R_m}{l_i R_i} + (p+q+1)\frac{b_o R_m}{l_o R_o}\right]\left[\left(\frac{m-1}{2}\right)^{1/2}\delta_{p,m-1} + \left(\frac{m+1}{2}\right)^{1/2}\delta_{p,m+1}\right]\delta_{q,n}\right\}.$$

R is diagonal to zeroth order. The lowest order correction couples m with $m\pm1$, $m\pm3$ in the X-direction and n with n, $n\pm2$ in the Y-direction. The reflection matrix is not symmetric, $R^{mn}_{pq} \neq R^{pq}_{mn}$. Also, it is not invariant to interchanging X and Y. This means that the modes $u_{mn}(x,y)$ and $u_{nm}(x,y)$ with $m \neq n$ are reflected differently.

Appendix B. Computation of the First Matrix Elements in Laguerre Representation.

Representation using Gaussian-Laguerre modes may be advantageous in numerical simulations because fewer Laguerre modes than Hermite modes are required to represent close-to-axisymmetric radiation profiles with the same accuracy. However, the computation of Eqs. (33a) to (33e) is not so straightforward. The integrations (33a) and (33b) for I^{pq} and K^{pq} over the polar angle θ_s involve trigonometric functions of complicated arguments $\theta_i(\theta_s)$ and $\theta_o(\theta_s)$, given implicitly by Eq. (31b). There is no simple recurrence formula for this calculation. The first few elements are computed here by expansions in powers of $r_s/R_m < \zeta \sim \xi$. Substituting from (31b) inside (33) and renormalizing $r_s^2/2W_o^2 = X/(1-\sin^2\phi/2\sin^2\theta)$, one obtains, to first order in ξ,

$$D^{00}(X) = \int_o^{2\pi} d\theta \; \frac{1}{1-\sin^2\frac{\phi}{2}\sin^2\theta}, \tag{B0}$$

$$D^{10}(X) = -I^{01}(X) = \frac{1}{2\sqrt{2}}\,\xi\, X \tan\frac{\phi}{2} \int_o^{2\pi} d\theta \; \frac{\cos^2\theta}{\left(1-\sin^2\frac{\phi}{2}\sin^2\theta\right)^2}, \tag{B1}$$

$$D^{11}(X) = \int_o^{2\pi} d\theta \; \frac{\cos^2\theta}{\left(1-\sin^2\frac{\phi}{2}\sin^2\theta\right)^2}, \tag{B2}$$

$$D^{-1-1}(X) = \cos^2\frac{\phi}{2} \int_o^{2\pi} d\theta \; \frac{\sin^2\theta}{\left(1-\sin^2\frac{\phi}{2}\sin^2\theta\right)^2}, \tag{B3}$$

$$D^{-10}(X) = -D^{0-1}(X) = -\frac{1}{2\sqrt{2}}\,\xi\, X \tan\frac{\phi}{2} \int_o^{2\pi} d\theta \; \frac{\left(1-\cos^2\frac{\phi}{2}\tan^2\theta\right)\cos^2\theta}{\left(1-\sin^2\frac{\phi}{2}\sin^2\theta\right)^2}, \tag{B4}$$

$$D^{-11}(X) = D^{1-1}(X) = 0. \tag{B5}$$

We only need E^{pq} to zeroth order in ξ, obtaining

$$E^{-10}(X) = -E^{0-1}(X) = \int_0^{2\pi} d\theta \frac{\cos\frac{\phi}{2}\sin^2\theta}{\left(1-\sin^2\frac{\phi}{2}\sin^2\theta\right)^{3/2}}, \tag{B6}$$

and

$$E^{pq} = 0 + O(\xi) \qquad \text{for } (p,q) \neq (-1,0), (0-1). \tag{B7}$$

The integrals (B1) - (B7) are evaluated using the formula

$$\int_0^{\pi/2} dx \frac{\sin^{\mu}x \cos^{\nu}x}{\left(1-k^2\sin^2x\right)^{\rho}} = \frac{1}{2} B\left(\frac{\mu+1}{2}, \frac{\nu+1}{2}\right) F\left(\rho, \frac{\mu+1}{2}, \frac{\mu+\nu+2}{2}, k^2\right), \tag{B8}$$

where $B(p,q) = \Gamma(p)\Gamma(q)/\Gamma(p+q)$, Γ is the factorial function and F is the hypergeometric function. The radial integrations for U, V and W are performed directly, using the expressions $L_m^p(x)$ for the Laguerre functions and the identities

$$\int_0^{\infty} e^{-x} x^{-1/2} dx = \sqrt{\pi},$$

$$\int_0^{\infty} e^{-x} x^{n} dx = n!,$$

$$\int_0^{\infty} e^{-x} x^{n+1/2} dx = \frac{1}{2} \cdot \frac{3}{2} \ldots (n+1/2)\sqrt{\pi}. \tag{B9}$$

Again, we extend the limits of integration to infinity assuming $\rho\cos(\phi/2) >> W_i$ and $\alpha = 1$. The zeroth order contribution is given by

$$R_{00}^{00}(0) = 1,$$
$$R_{11}^{00}(0) = 1,$$

$$R^{-1-1}_{1\ 1}(0) = \cos^3 \frac{\phi}{2}\, F\left(2,\frac{3}{2},2,\sin^2 \frac{\phi}{2}\right),$$

$$R^{11}_{11}(0) = \cos \frac{\phi}{2}\, F\left(2,\frac{1}{2},2,\sin^2 \frac{\phi}{2}\right),$$

$$R^{11}_{00}(0) = \cos \frac{\phi}{2}\, F\left(2,\frac{1}{2},2,\sin^2 \frac{\phi}{2}\right),$$

$$R^{-1-1}_{0\ 0}(0) = \cos^2 \frac{\phi}{2}\, F\left(2,\frac{3}{2},2,\sin^2 \frac{\phi}{2}\right). \qquad \text{(B10)}$$

The first order corrections in ξ are given by

$$R^{10}_{00}(1) = -R^{01}_{00}(1) = \left(\frac{\pi}{2}\right)^{1/2} \frac{3}{8} \sin \frac{\phi}{2}\, F\left(2,\frac{1}{2},2,\ \sin^2 \frac{\phi}{2}\right),$$

$$R^{10}_{01}(1) = -R^{01}_{10}(1) = \left(\frac{\pi}{2}\right)^{1/2} \frac{9}{16} \sin \frac{\phi}{2}\, F\left(2,\frac{1}{2},2,\ \sin^2 \frac{\phi}{2}\right),$$

$$R^{00}_{01}(1) = R^{00}_{10}(1) = 0,$$

$$R^{10}_{10}(1) = -R^{01}_{01}(1) = \left(\frac{\pi}{2}\right) \quad \frac{3^{1/2}}{16} \sin \frac{\phi}{2}\, F\left(2,\frac{1}{2},2,\ \sin^2 \frac{\phi}{2}\right),$$

$$R^{10}_{11}(1) = -R^{01}_{11}(1) = -\left(\frac{\pi}{2}\right)^{1/2} \frac{39}{32} \sin \frac{\phi}{2}\, F\left(2,\frac{1}{2},2,\ \sin^2 \frac{\phi}{2}\right), \qquad \text{(B11)}$$

and

$$R^{-10}_{00}(1) = \sin \frac{\phi}{2} \left\{ \pm \left[\left(\frac{\pi}{2}\right)^{1/2} \frac{3}{8}\, F\left(2,\frac{1}{2},2,\ \sin^2 \frac{\phi}{2}\right) - \cos^2 \frac{\phi}{2}\, F\left(2,\frac{3}{2},2,\ \sin^2 \frac{\phi}{2}\right) \right] \right.$$

$$\left. \pm \frac{1}{2} \cos^2 \frac{\phi}{2}\, F\left(\frac{3}{2},\frac{3}{2},2,\ \sin^2 \frac{\phi}{2}\right) \begin{bmatrix} -4.5 & + i2^{-1/2} \\ -3.5 & + i2^{-1/2} \end{bmatrix} \right\},$$

$$R^{-10}_{01}(1) = \sin \frac{\phi}{2} \left\{ \pm \left[\left(\frac{\pi}{2}\right)^{1/2} \frac{9}{16}\, F\left(2,\frac{1}{2},2,\ \sin^2 \frac{\phi}{2}\right) - \cos^2 \frac{\phi}{2}\, F\left(2,\frac{3}{2},2,\ \sin^2 \frac{\phi}{2}\right) \right] \right.$$

$$\left. \pm \frac{1}{2} \cos^2 \frac{\phi}{2}\, F\left(\frac{3}{2},\frac{3}{2},2,\ \sin^2 \frac{\phi}{2}\right) \left[2 - i\, 2^{-1/2}\right] \right\},$$

$$R^{-10}_{11}(1) = \sin\frac{\phi}{2}\left\{\pm\left[\left(\frac{\pi}{2}\right)^{1/2}\frac{39}{32}F\left(2,\frac{1}{2},2,\sin^2\frac{\phi}{2}\right) - \cos^2\frac{\phi}{2}F\left(2,\frac{3}{2},2,\sin^2\frac{\phi}{2}\right)\right],\right.$$

$$\left.\pm\frac{1}{2}\cos^2\frac{\phi}{2}F\left(\frac{3}{2},\frac{3}{2},2,\sin^2\frac{\phi}{2}\right)\begin{bmatrix}4.5 + i2^{-1/2}\\ 3.5 + i2^{-1/2}\end{bmatrix}\right\}. \qquad \text{(B12)}$$

The (-) sign and the lowest row inside the last square bracket in (B12) correspond to exchanging indices,

$$R^{pq}_{mn} \leftrightarrow R^{qp}_{nm}.$$

Note also that the elements $R^{1-1}_{m\ n}$, R^{-11}_{mn}, coupling sine and cosine modes, are of order ξ^2 or higher for every m, n,

$$R^{-1\ 1}_{m\ n} \sim O(\xi^2). \qquad \text{(B13)}$$

Appendix C. Computation of the Cross-Polarization Matrix Elements

We compute here some of the first order cross-polarization matrix elements in case of large mirror size $\rho >> W_i$ and $\alpha \to 1$. In the Gaussian-Hermite representation we find from (44b), using the notation of Appendix A,

$$G^{mn}_{pq} = 2^m m!\ \sqrt{\pi}\ \langle Y \rangle_{q,n} \delta_{p,m}$$

$$= \pi\ 2^m m!\ \left\{ 2^{n-1} n!\ \delta_{q,n-1} + 2^n\ (n+1)!\ \delta_{q,n+1} \right\} \delta_{p,m}, \qquad (C1)$$

yielding

$$Q^{mn}_{pq}\ (1) = \xi \sin \frac{\phi}{2} \left\{ \sqrt{n}\ \delta_{q,n-1} + \sqrt{n+1}\ \delta_{q,n+1} \right\} \delta_{p,m}. \qquad (C2)$$

In Gaussian-Laguerre representation we only have to compute $B^{pq}(X)$, Eq. (45c), to zeroth order in ξ. Applying the methods of Appendix B, we find

$$B^{pq} = O(\xi), \text{ if } p,q \neq (1,0),\ (0,1),$$

$$B^{10} = B^{01} = \int_0^{2\pi} \frac{d\theta \cos^2\theta}{\left(1 - \sin^2 \frac{\phi}{2} \sin^2\theta\right)^{3/2}}. \qquad (C3)$$

Noting that $G_{mn}(X)$ is the same as $W^{pq}_{mn}(X)$, Eq. (33e), and inserting (C3) and (33e) inside (45a), we obtain

$$Q^{10}_{10}\ (1) = Q^{01}_{01}\ (1) = 0,$$

$$Q^{10}_{00}\ (1) = Q^{01}_{00}\ (1) = \xi \sin \frac{\phi}{2}\ F\left(\frac{3}{2},\ \frac{1}{2},\ 2,\ \sin^2 \frac{\phi}{2}\right),$$

$$Q^{10}_{01}(1) = Q^{01}_{10}(1) = -\xi \sin \frac{\phi}{2}\ F\left(\frac{3}{2},\ \frac{1}{2},\ 2,\ \sin^2 \frac{\phi}{2}\right),$$

$$Q^{10}_{11}\ (1) = Q^{01}_{11}\ (1) = \sqrt{2}\ \xi \sin \frac{\phi}{2}\ F\left(\frac{3}{2},\ \frac{1}{2},\ 2,\ \sin^2 \frac{\phi}{2}\right). \qquad (C4)$$

Appendix D. Small Aperture Limit

We have seen in Sec. V that in case of mirror surface S_1 with an aperture of area S_2 the reflection matrix is given by

$$R(S;W_o) = R(S_1;W_o) - R(S_2;W_o) \tag{D1}$$

In case that $S_2 << S_1$ the spot size W_o optimizing the representation for the scattered radiation will be determined predominantly by the surface S_1. Thus, the formula (23) with W_o given from

$$\frac{\partial R(S_1;\alpha)}{\partial \alpha} = 0, \tag{D2}$$

can be used for the modal decomposition of the scattered radiation. According to Eqs. (28a) and (29a) for the Hermite representation, and Eqs. (32a) and (33c) for the Laguerre representation, the lowest order contribution from a small aperture $\rho_2 << W_o$ scales as $R(S_2;W_o) \sim \xi^2$.

In some cases, however, it is important to know the <u>total</u> radiation diffracted through a small hole, rather than the modal decomposition. In case of small apperture ρ_2,

$$\rho_2^2 << l_o k^{-1} \quad \text{or} \quad \lambda >> \rho_2^2/l_o, \tag{D3}$$

where $l_o \sim z$ is the distance of the observation point from the mirror, the paraxial approximation, Eq. (8b) is taken one step further, setting

$$\frac{k}{z-z_o}\left[\left(x-x_o\right)^2 + \left(y-y_o\right)^2\right] \simeq \frac{k}{z-z_o}\left[\left(x^2+y^2\right) - 2xx_o - 2yy_o\right]. \tag{D4}$$

Substituting (D4) inside (8a) we obtain the "far field" limit of the diffracted radiation

$$A^o(x,y,z=0) = \frac{ik}{2\pi z_o}\int dx_o \int dy_o A^i(x_o,y_o)(\hat{n}\cdot\delta\hat{r})$$

$$\exp\left\{-\frac{ik}{2z_o}\left[\left(x^2+y^2\right) - 2xx_o - 2yy_o\right]\right\}, \qquad (D5)$$

also known as Fraunhoffer diffraction. The condition (D3) can only be valid for appertures much smaller than the spot size W_o at the mirror, $\rho_2 \ll W_o$, since for $\rho_2 \sim W_o$ (D3) is violated, $k\rho_2^2 \sim kW_o^2 \sim kw_o^2\,(1+l_o^2/b_o^2) \sim b_o(1+l_o^2/b_o^2) > l_o$. Neglecting terms of order $kx_m^2/l_o \sim k\rho_2^2/l_o \ll 1$ means that terms of order x_s/l_m, $x_s/l_o \ll 1/kx_s$, where $kx_s > 1$, must also be neglected. The source term can be written as $A^i[x_i,y_i] \simeq A^i[x_s,y_s]$. Rescaling variables to

$$K_x = \cos\frac{\phi}{2}\,\frac{kx}{l_o}, \qquad K_y = \frac{ky}{l_o} \qquad (D6)$$

we obtain

$$A^o(x,y,0) = e^{i(pq_o + k\frac{x^2+y^2}{l_o})}\cos\frac{\phi}{2}\,\frac{ik}{2\pi l_o}\int dx_s\int dy_s A^i(x_s,y_s)e^{iK_xx_s+iK_yy_s}. \qquad (D7)$$

According to (D7) the outgoing radiation is the Fourier transform of the incoming radiation in respect to K_x, K_y. Defining the "polar" coordinates $K = (K_x^2+K_y^2)^{1/2}$, $\Theta = \tan^{-1}(K_x/K_y)$, we obtain, for $A^i(x_s,y_s)$ $= \sum_{K,l} C^i_{pq}\,u_{pq}(x_s,y_s)$, the scattered radiation

$$A^o(x,y,0) = \sum_{p,q} c^i_{pq}\,\frac{ika_{pq}}{2\pi l_o}\,e^{ik\left(l_o + \frac{x^2+y^2}{2l_o}\right)}\ X$$

$$\cos\frac{\phi}{2}\int dx_s\int dy_s\, H_p\left[\sqrt{2}\,\frac{x_s}{W_i}\cos\frac{\phi}{2}\right]H_q\left[\sqrt{2}\,\frac{y_s}{W_i}\right] e^{-\frac{x_s^2\cos^2\frac{\phi}{2}+y_s^2}{W_i^2}}$$

$$\sum_{m=-\infty}^{\infty}\sum_{n=-\infty}^{\infty} J_n(Kx_s)\,J_m(Ky_s)\,e^{i(m-n)\Theta}\,i^{m+n}\,e^{in\frac{\pi}{2}}. \qquad (D8)$$

The zeroth order contribution in $x_s/W_i << 1$ yields

$$A^o(x,y,0) \simeq c_{oo}^i\,\frac{ika_{oo}}{2\pi l_o}\,e^{ik\left(l_o+\frac{x^2+y^2}{2l_o}\right)}$$

$$X\cos\frac{\phi}{2}\int dx_s\int dy_s\, J_o(Kx_s)\,J_o(Ky_s)\,e^{-\frac{x_s^2\cos^2\frac{\phi}{2}+y_s^2}{W_i^2}}. \qquad (D9)$$

The waist size w_f for the Fraunhoffer modes is given by the zeros of the Bessel functions

$$K(w_f)\,x_s \sim \frac{kw_f}{l_o}\,\rho_2 \sim 2\pi. \qquad (D10)$$

Therefore, the diffraction angle θ_f is

$$\theta_f \simeq \frac{w_f}{l_o} \sim \frac{\lambda}{\rho_2}. \qquad (D11)$$

The requirement $\theta_f << 1$ for the validity of the paraxial approximation puts a lower limit in the aperture size ρ_2

$$\rho_2 >> \lambda. \qquad (D12)$$

In case the aperture size is of the order of the wavelength λ the scattered wavefunctions are spherical rather than Gaussian. Because the overall effect of a scatterer with size $\rho_2 \sim \lambda$ is very small, the familiar from quantum mechanics Born approximation, involving perturbation theory, is applicable in that case.

Acknowledgements

This work was supported by the Strategic Defense Initiative Organization and managed by the U. S. Army Strategic Defense Command.

References

1. L. R. Elias, W. M. Fairbanks. J. M. J. Madey, H. A. Schwettman and T. I. Smith, Phys. Rev. Lett. 36, 717 (1976).
2. T. I. Smith, H. A. Schwettman, R. Rohatgi, Y. Lapierre and J. Edighoffer in Proceedings of the Eighth International FEL Conference, Glasgow, Scotland, edited by M. Poole (North Holland, Amsterdam, 1987), p. 1.
3. R. W. Warren, D. W. Feldman, B. E. Newnam, S. C. Bender, W. E. Stein, A. H. Lumpkin, R. A. Lohsen, J. G Goldstein, B. D. McVey and K. C. D. Chan, in Proceedings of the Eighth International FEL Conference, Glasgow, Scotland, edited by M. Poole (North Holland, Amsterdam, 1987), p. 8.
4. K. E. Robinson, T. L. Churchill, D. C. Quimby, D. M. Shemwell, J. M. Slater, A. S. Valla, A. A. Vetter, J. Adamski, T. Doering, W. Gallagher, R. Kennedy, B. Robinson, D. Shoffstall, E. Tyson, A. Vetter and A. Yeremian in Proceedings of the Eighth International FEL Conference, Glasgow, Scotland, edited by M. Poole (North Holland, Amsterdam, 1987), p. 49.
5. M. Billardon, P. Elleaume, J. M. Ortega, C. Bazin, M. Bergher, M. E. Couprie, Y. Lapierre, Y. Petroff, P. Prazeres and M. Velghe, in Proceedings of the Eighth International FEL Conference, Glasgow, Scotland, edited by M. Poole (North Holland, Amsterdam, 1987), p. 72.
6. T. Masud, T. C. Marshall, S. P. Schlesinger and F. G. Yee, Phys. Rev. Lett. 56, 1567 (1986).
7. X. K. Maruyama, S. Penner, C. M. Tang and P. Sprangle, in Proceedings of the Eighth International FEL Conference, Glasgow, Scotland, edited by M. Poole (North Holland, Amsterdam, 1987), p. 259.

8. S. Solimeno and A. Torre, Nucl. Instr. and Methods A237, 404 (1985).

9. J. A. Murphy, Intl. J. Infrared and Millimeter Waves 8, 1165 (1987).

10. See, for example, H. A. Hauss in Waves and Fields in Optoelectronics, (Prentice Hall, New Jersey, 1984), p. 180, and references therein.

11. P. Sprangle, A. Ting and C. M. Tang, Phys. Rev. Lett. 59, 202 (1987).

12. P. Sprangle, A. Ting and C. M. Tang, Phys. Rev. A36, 2773 (1987).

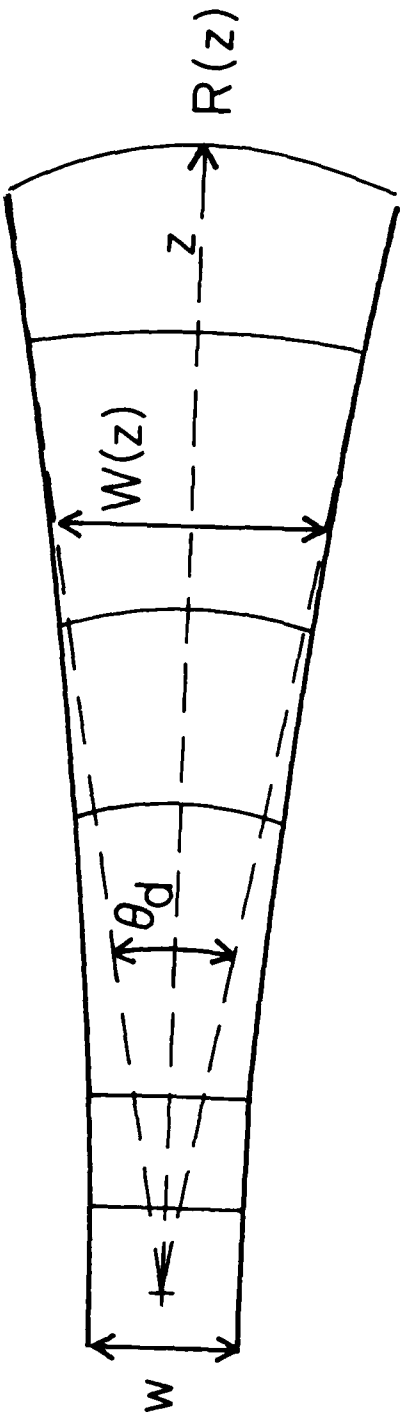

Figure 1 Schematic illustration of the radiation envelope for a Gaussian eigenmode.

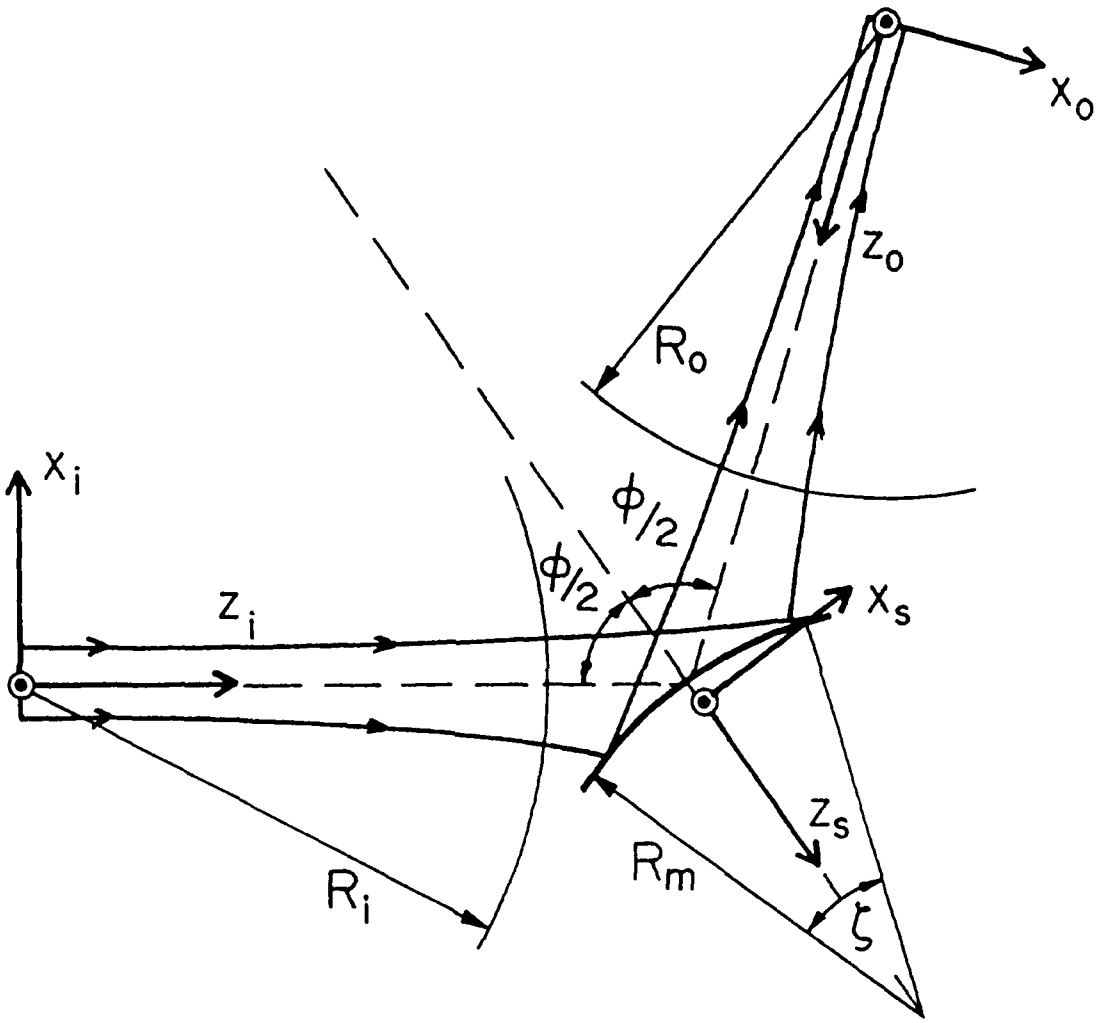

Figure 2 Reflection geometry.

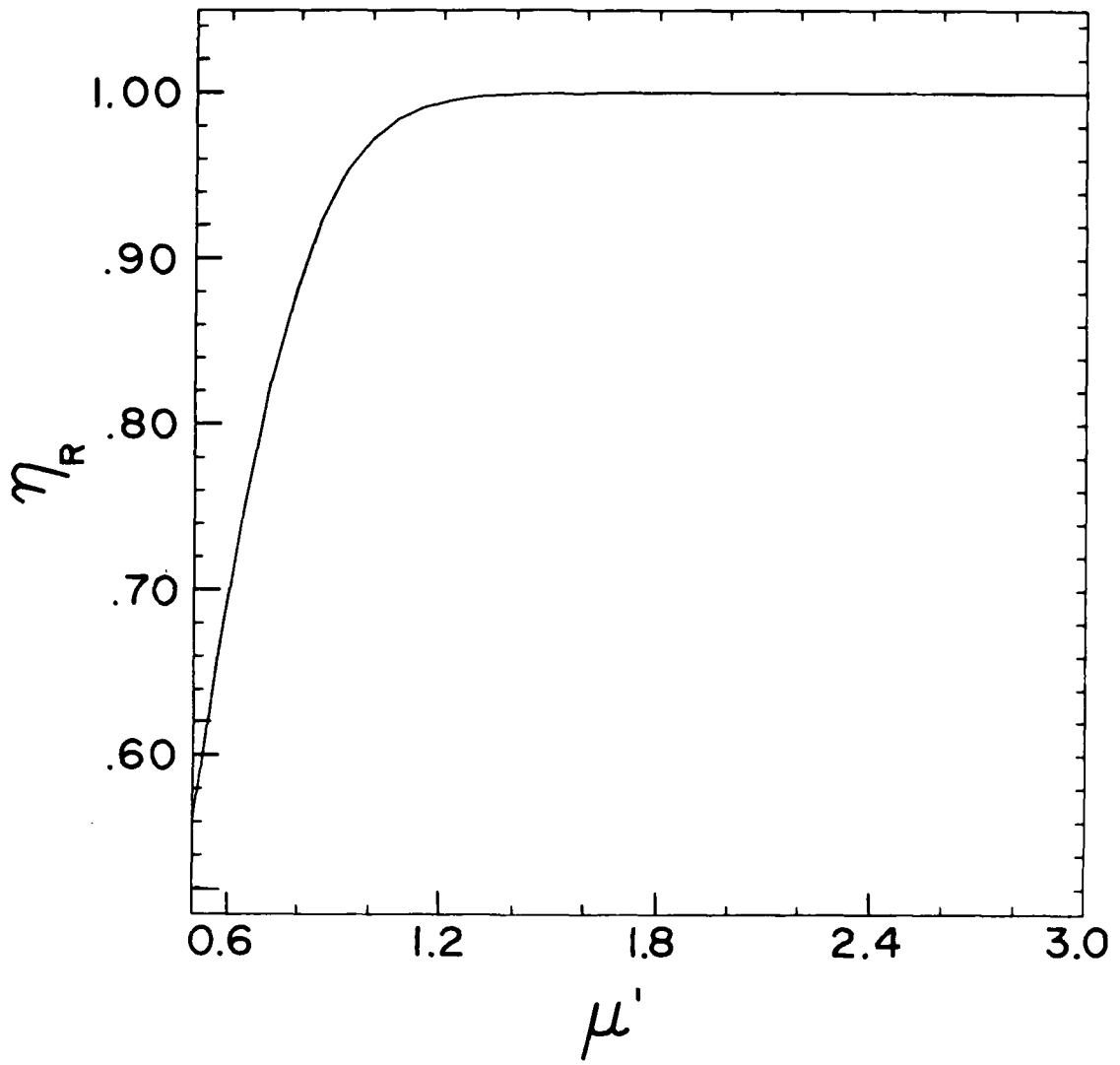

Figure 3 Plot of the total reflection coefficient η_R for the lowest order mode as a function of the mirror size μ' for $\phi = 90°$. The radiation has wavelength $\lambda = 10^{-4}$cm, waist $w_i = 2\times10^{-1}$cm at distance $l_i = 1.8\times10^{2}$cm from the mirror and radius of curvature $R_i = R_m = 8.95\times10^{3}$cm.

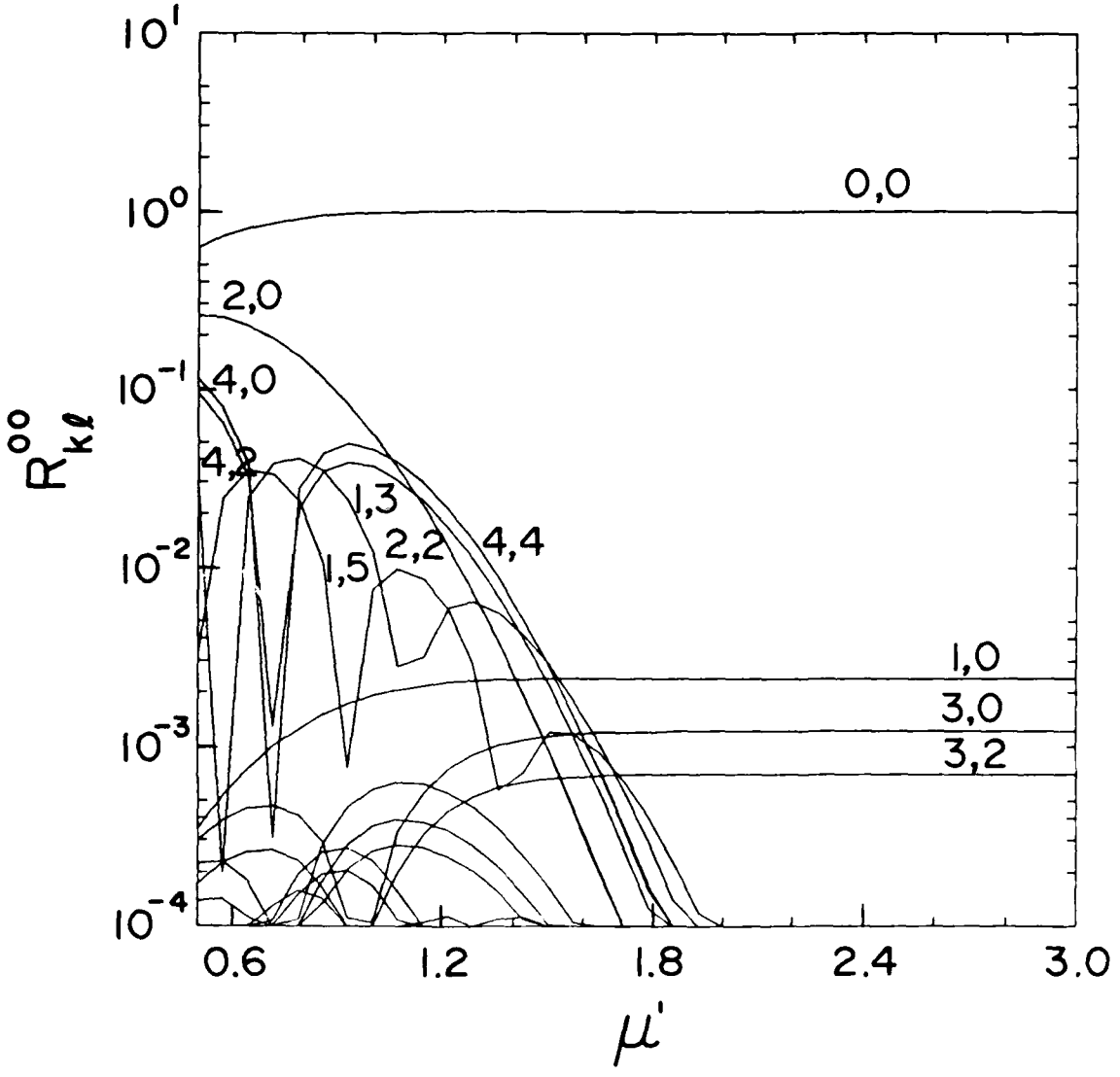

Figure 4 Reflection matrix elements for the lowest order mode (0,0) into the first 25 modes (p,q) against the relative mirror size μ'. The magnitude $|R^{00}_{pq}|$ is plotted for angle of deflection $\phi = 90°$, $\alpha = 1$ ($W_i = W_o$).

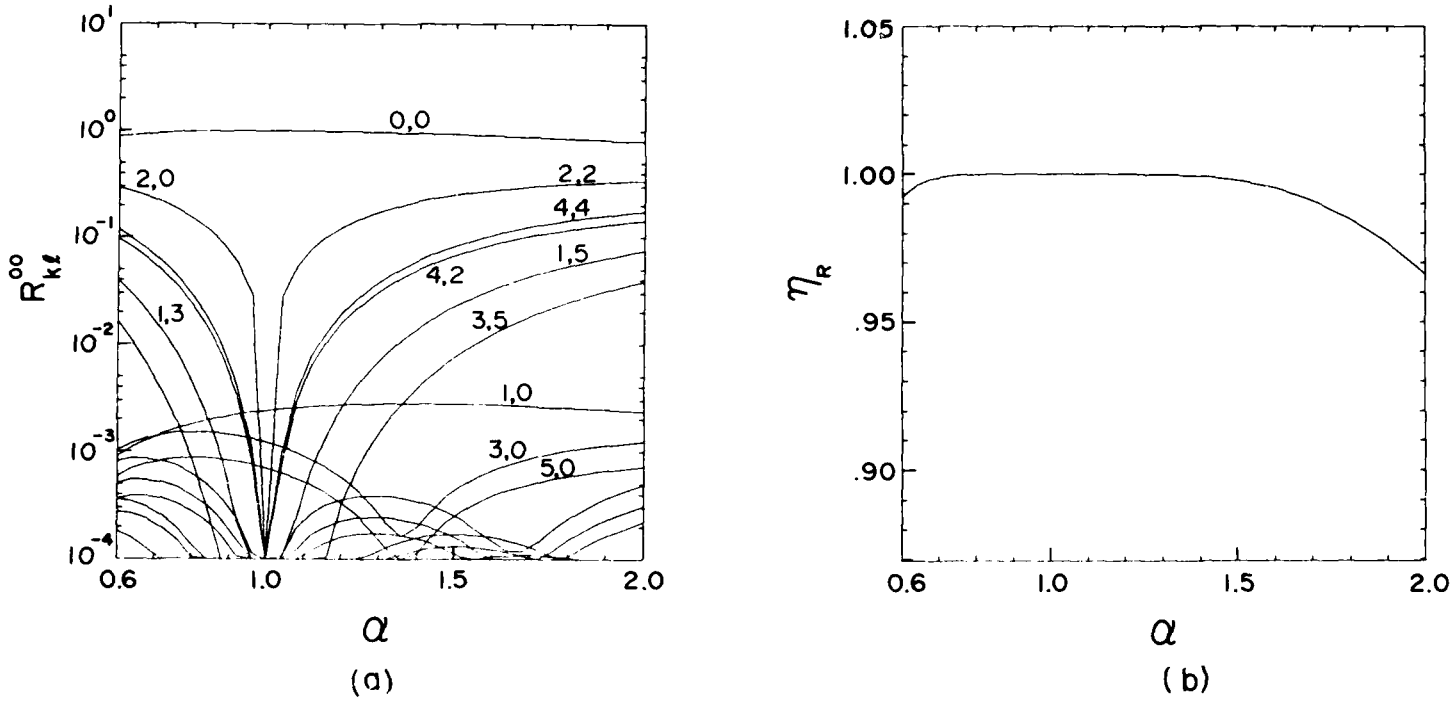

Figure 5 Plots of the reflection matrix elements $|R^{00}_{pq}|$ against the spot size ratio α for $\mu' = 2$ and $\phi = 90°$. Radiation parameters are the same as in Fig. 3.

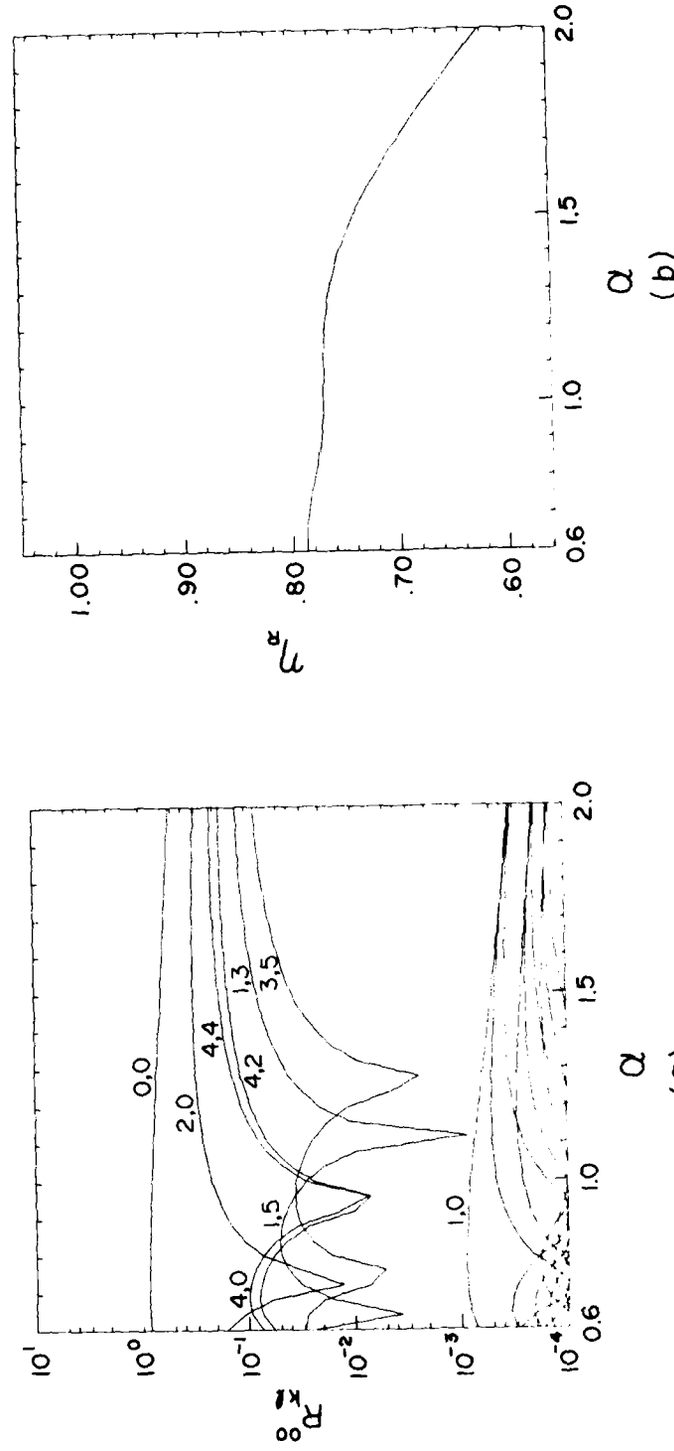

Figure 6 Same as in Fig. 5 for μ' = 0.66.

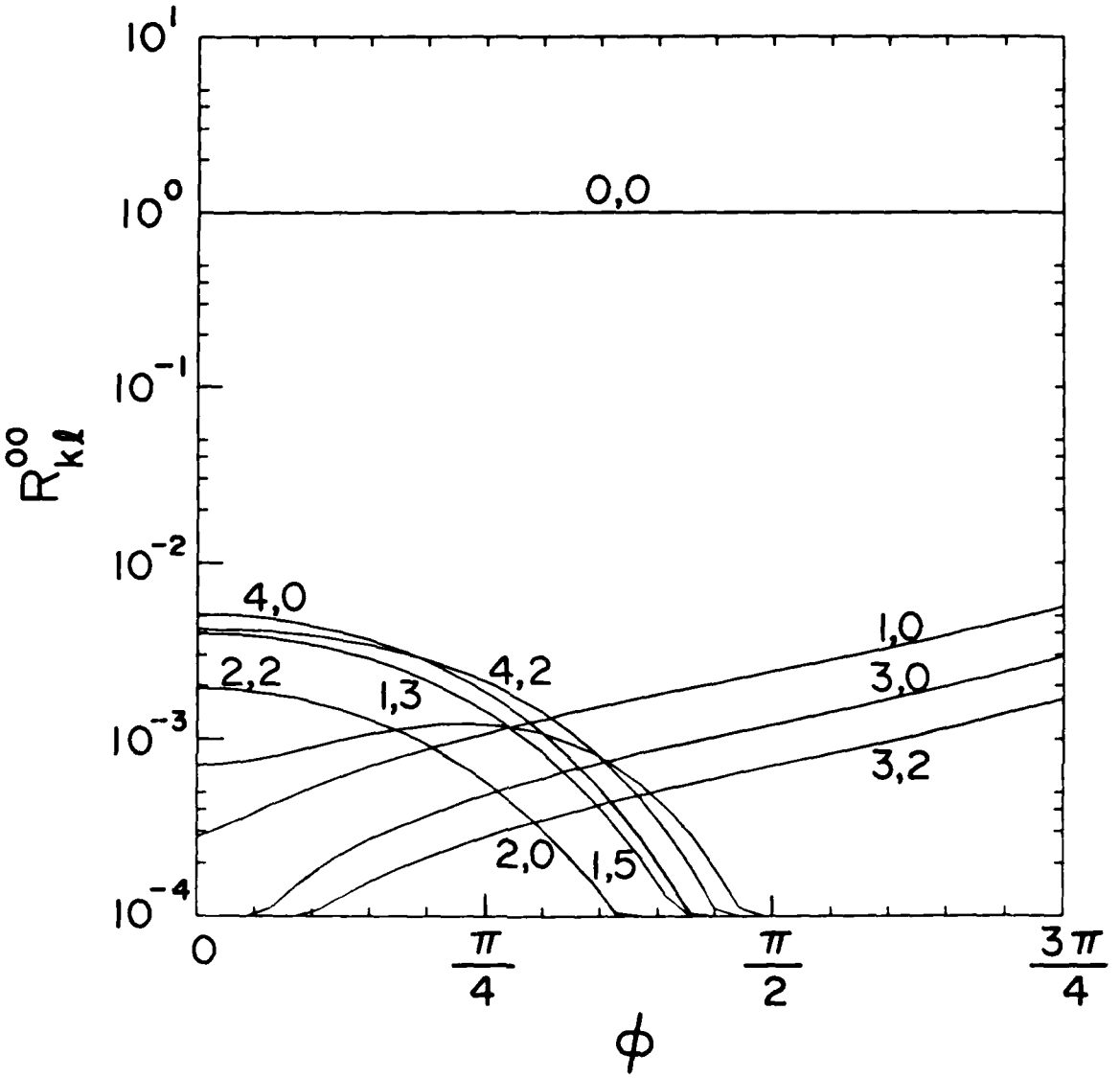

Figure 7 Plots of the reflection matrix elements $|R^{00}_{pq}|$ against the angle of deflection ϕ for $\mu' = 2$ and $\alpha = 1$.

DISTRIBUTION LIST*

Naval Research Laboratory
4555 Overlook Avenue, S.W.
Washington, DC 20375-5000

Attn: Code 1000 - Commanding Officer, CAPT W. G. Clautice
1001 - Dr. T. Coffey
1005 - Head, Office of Management & Admin.
1200 - CAPT M. A. Howard
1220 - Mr. M. Ferguson
2000 - Director of Technical Services
2604 - NRL Historian
4000 - Dr. W. R. Ellis
4600 - Dr. D. Nagel
4603 - Dr. W. W. Zachary
4700 - Dr. S. Ossakow (26 copies)
4700.1-Dr A. W. Ali
4710 - Dr. C. A. Kapetanakos
4730 - Dr. R. Elton
4740 - Dr. W. M. Manheimer
4740 - Dr. W. Black
4740 - Dr. J. Condon
4740 - Dr. A. W. Fliflet
4740 - Dr. S. Gold
4740 - Dr. D. L. Hardesty
4740 - Dr. A. K. Kinkead
4740 - Dr. M. Rhinewine
4770 - Dr. G. Cooperstein
4790 - Dr. P. Sprangle (20 copies)
4790 - Dr. C. M. Tang (20 copies)
4790 - Dr. M. Lampe
4790 - Dr. Y. Y. Lau
4790A- W. Brizzi
5700 - Dr. L. A. Cosby
6840 - Dr. S. Y. Ahn
6840 - Dr. A. Ganguly
6840 - Dr. R. K. Parker
6843 - Dr. R. H. Jackson
6843 - Dr. N. R. Vanderplaats
6875 - Dr. R. Wagner
2628 - Documents (22 copies)
2634 - D. Wilbanks

* Every name listed on distribution gets one copy except for those where extra copies are noted.

Dr. R. E. Aamodt
Science Appl. Intl. Corp.
1515 Walnut Street
Boulder, CO 80302

Dr. J. Adamski
Boeing Aerospace Company
P.O. Box 3999
Seattle, WA 98124

Dr. H. Agravante
TRW, Inc.
One Space Park
Redondo Beach, CA 90278 / R1-2020

Prof. I. Alexeff
University of Tennessee
Dept. of Electrical Engr.
Knoxville, TN 37916

Dr. L. Altgilbers
3805 Jamestown
Huntsville, AL 35810

Dr. A. Amir
Quantum Inst. and Dept. of Physics
University of California
Santa Barbara, CA 93106

Dr. Bruce Anderson
Air Force Weapons Laboratory
Kirtland AFB
Albuquerque, NM 87117

Dr. Antonio Anselmo
VARIAN
MS K-416
611 Hanson Way
Palo Alto, CA 94303

Dr. T. M. Antonsen
University of Maryland
College Park, MD 20742

Dr. C. M. Armstrong
Code 6843
Naval Research Laboratory
Washington, DC 20375-5000

Dr. Tony Armstrong
Science Applications Intl. Corp.
P.O. Box 2351
La Jolla, CA 92038

Assistant Secretary of the
Air Force (RD&L)
Room 4E856, The Pentagon
Washington, D.C. 20330

Dr. W. P. Ballard
Sandia National Laboratories
ORG. 1231, P.O. Box 5800
Albuquerque, NM 87185

Mr. Jon Barber
Dept. of Physics
Bethel College
St. Paul, MN 55112

Dr. W. A. Barletta
Lawrence Livermore National Lab.
P. O. Box 808
Livermore, CA 94550

Dr. L. R. Barnett
3053 Merrill Eng. Bldg.
University of Utah
Salt Lake City UT 84112

Commander George Bates, PMS 405-300
Naval Sea Systems Command
Department of the Navy
Washington, DC 20362

Dr. Latika Becker
U. S. Army SDC
DASD-H-F
P. O. Box 1500
Huntsville, AL 35807-3801

Dr. W. Becker
Univ. of New Mexico
Institute for Mod. Opt.
Albuquerque, NM 87131

Dr. Robert Behringer
Code 818
Office of Naval Research
1030 E. Green
Pasadena, CA 91106

Dr. G. Bekefi (5 copies)
Mass. Institute of Tech.
Bldg. 26
Cambridge, MA 02139

Dr. S. Bender
Los Alamos National Laboratory
P. O. Box 1663
Los Alamos, NM 87545

Dr. J. Benford
Physics International
2700 Merced Street
San Leandro, CA 94577

Dr. Herbert S. Bennett
National Bureau of Standards
Bldg. 225, Rm. A352
Washington, DC 20234

Dr. T. Berlincourt
Office of Naval Research
Attn: Code 420
Arlington, VA 22217

Dr. I. B. Bernstein (10 copies)
Mason Laboratory
Yale University
400 Temple Street
New Haven, CT 06520

Dr. Vladislav Bevc
Synergy Research Institute
P.O. Box 561
San Ramon, CA 94583

Dr. Anup Bhowmik
Rockwell International/Rocketdyne Div.
6633 Canoga Avenue, FA-40
Canoga Park, CA 91304

Dr. K. Jim Bickford
RDA
2301F Yale Blvd., S.E.
Albuquerque, NM 87106

Dr. D. L. Birx
Lawrence Livermore National Laboratory
P. O. Box 808
Livermore, CA 94550

Dr. J. Bisognano
Lawrence Berkeley Laboratory
University of California, Berkeley
Berkeley, CA 94720

Dr. Steve Bitterly
Rockwell International/Rocketdyne Div.
6633 Canoga Avenue, FA-40
Canoga Park, CA 91304

Dr. H. Boehmer
TRW DSSG
One Space Park
Redondo Beach, CA 90278

Dr. I. Boscolo
Quantum Institute
University of California
Santa Barbara, CA 93106

Dr. B. Boswell
Lab for Laser Energetics
University of Rochester
250 E. River Road
Rochester, NY 14623

Dr. G. Bourianoff
1901 Rutland Drive
Austin, TX 78758

Dr. J. K. Boyd
Lawrence Livermore National Laboratory
P. O. Box 808
Livermore, CA 94550

Dr. H. Brandt
Department of the Army
Harry Diamond Laboratory
2800 Powder Mill Rd.
Adelphi, MD 20783

Dr. Charles Brau (2 copies)
Los Alamos National Laboratory
P.O. Box 1663, M.S. - 817
Los Alamos, NM 87545

Dr. R. Briggs
Lawrence Livermore National Lab.
Attn: (L-71)
P.O. Box 808
Livermore, CA 94550

Dr. D. L. Bullock
Optical Sciences Department
TRW Space and Technology Group
Redondo Beach, CA 90278

Dr. Fred Burskirk
Physics Department
Naval Postgraduate School
Monterey, CA 93940

Dr. Ken Busby
Mission Research Corporation
1720 Randolph Road, S.E.
Albuquerque, NM 87106

Dr. K. J. Button
Francis Bitter Natl. Magnet Lab.
M. I. T. Branch, Box 72
Cambridge, MA 02139-0901

Dr. J. A. Byers
Lawrence Livermore National Lab.
Attn: (L-630)
P. O. Box 808
Livermore, CA 94550

Dr. Gregory Canavan
Office of Inertial Fusion
U.S. Dept. of Energy
M.S. C404
Washington, DC 20545

Dr. Malcolm Caplan
4219 Garland Drive
Fremont, CA 94536

Dr. Maria Caponi
TRW, Building R-1, Room 1184
One Space Park
Redondo Beach, CA 90278

Dr. B. Carlsten
Los Alamos National Laboratory
P. O. Box 1663
Los Alamos, NM 87545

Dr. A. Carmichael
U. S. Army - FTC
P. O. Box 1500
Huntsville, AL 35807-3801

Dr. J. Cary
University of Colorado
Box 391
Boulder, CO 80309

Prof. William Case
Dept. of Physics
Grinnell College
Grinnell, IA 50112

Mr. Charles Cason
U. S. Army Strategic Def. Command
ATTN: Code CSSD-H-D
P. O. Box 1500
Huntsville, AL 35807-3801

Dr. R. Center
Math. Sci. NW., Inc.
2755 Northup Way
Bellevue, WA 98004

Prof. Frank Chan
School of Eng. & Applied Sciences
Univ. of Calif. at Los Angeles
7731 K Boelter Hall
Los Angeles, CA 90024

Dr. K. C. Chan
Los Alamos National Laboratory
P. O. Box 1663
Los Alamos, NM 87545

Dr. V. S. Chan
GA Technologies
P.O. Box 85608
San Diego, CA 92138

Dr. Will E. Chandler
Pacific Missile Test Center
Code 0141-5
Point Muga, CA 93042

Dr. J. Chase
Lawrence Livermore National Laboratory
P. O. Box 808
Livermore, CA 94550

Dr. S. Chattopadhyay
Lawrence Berkeley Laboratory
University of California, Berkeley
Berkeley, CA 94720

Dr. S. Chen
MIT Plasma Fusion Center
NW16-176
Cambridge, MA 01890

Dr. Yu-Juan Chen
L-626
Lawrence Livermore National Laboratory
P. O. Box 808
Livermore, CA 94550

Dr. D. P. Chernin
Science Applications Intl. Corp.
1720 Goodridge Drive
McLean, VA 22102

Dr. Art Chester
Hughes E51
Mail Stop A269
P.O. Box 902
El Segundo, CA 90245

Dr. S. C. Chiu
GA Technologies Inc.
P.O. Box 85608
San Diego, CA 92138

Dr. Y. C. Cho
NASA-Lewis Research Center
Mail Stop-54-5
Cleveland, Ohio 44135

Dr. J. Christiansen
Hughes Aircraft Co.
Electron Dynamics Division
3100 West Lomita Blvd.
Torrance, CA 90509

Dr. T. L. Churchill
Spectra Technology, Inc.
2755 Northup Way
Bellevue, WA 98004

Major Bart Clare
USASDC
P. O. BOX 15280
Arlington, VA 22215-0500

Dr. Melville Clark
8 Richard Road
Wayland, MA 01778

Dr. Robert Clark
P.O. Box 1925
Washington, D.C. 20013

Dr. Alan J. Cole
TRW
One Space Park
Redondo Beach, CA 90278

Dr. William Colson
Berkeley Research Asso.
P. O. Box 241
Berkeley, CA 94701

Dr. William Condell
Office of Naval Research
Attn: Code 421
800 N. Quincy St.
Arlington, VA 22217

Dr. Richard Cooper
Los Alamos National Scientific
Laboratory
P.O. Box 1663
Los Alamos, NM 87545

Dr. Robert S. Cooper
Director, DARPA
1400 Wilson Boulevard
Arlington, VA 22209

Dr. M. Cornacchia
Lawrence Berkeley Laboratory
University of California, Berkeley
Berkeley, CA 94720

Dr. R. A. Cover
Rockwell International/Rocketdyne Div.
6633 Canoga Avenue, FA-38
Canoga Park, CA 91304

Dr. D. Crandall
ER-55, GTN
Department of Energy
Washington, DC 20545

Dr. Bruce Danly
MIT
NW16-174
Cambridge, MA 02139

Dr. R. Davidson (5 copies)
Plasma Fusion Center
Mass. Institute of Tech.
Cambridge, MA 02139

Dr. John Dawson (4 copies)
Physics Department
University of California
Los Angeles, CA 90024

Dr. David A. G. Deacon
Deacon Research
Suite 203
900 Welch Road
Palo Alto, CA 94306

Dr. Philip Debenham
Center for Radiation Research
National Bureau of Standards
Gaithersburg, MD 20899

Dr. T. L. Deloney
Dept. of Electrical Engineering
Stanford University
Stanford, CA 94305

Deputy Under Secretary of
Defense for R&AT
Room 3E114, The Pentagon
Washington, D.C. 20301

Prof. P. Diament
Dept. of Electrical Engineering
Columbia University
New York, NY 10027

Dr. N. Dionne
Raytheon Company
Microwave Power Tube Division
Foundry Avenue
Waltham, MA 02154

Director
National Security Agency
Fort Meade, MD 20755
ATTN: Dr. Richard Foss, A42
Dr. Thomas Handel, A243
Dr. Robert Madden, R/SA

Director of Research (2 copies)
U. S. Naval Academy
Annapolis, MD 21402

Dr. T. Doering
Boeing Aerospace Company
P.O. Box 3999
Seattle, WA 98124

Dr. Gunter Dohler
Northrop Corporation
Defense Systems Division
600 Hicks Road
Rolling Meadows, IL 60008

Dr. Franklin Dolezal
Hughes Research Laboratory
3011 Malibu Canyon Rd.
Malibu, CA 90265

Dr. A. Drobot
Science Applications Intl. Corp.
1710 Goodridge Road
McLean, VA 22102

Dr. Dwight Duston
Strategic Defense Initiative Org.
OSD/SDIO/IST
Washington, DC 20301-7100

Dr. Joseph Eberly
Physics Department
Univ. of Rochester
Rochester, NY 14627

Dr. Jim Eckstein
VARIAN
MS K-214
611 Hanson Way
Palo Alto, CA 94303

Dr. J. A. Edighoffer
TRW, Bldg. R-1
One Space Park
Redondo Beach, CA 90278

Dr. O. C. Eldridge
University of Wisconsin
1500 Johnson Drive
Madison, WI 53706

Dr. Luis R. Elias (2 copies)
Creol-FEL Research Pavillion
Suite 400
12424 Research Parkway
Orlando, FL 32826

Dr. C. J. Elliott
Los Alamos National Laboratory
P. O. Box 1663
Los Alamos, NM 87545

Dr. James Elliott
X1-Division, M.S. 531
Los Alamos Natl. Scientific Lab.
P. O. Box 1663
Los Alamos, NM 87545

Dr. A. England
Oak Ridge National Laboratory
P.O. Box Y
Mail Stop 3
Building 9201-2
Oak Ridge, TN 37830

Dr. William M. Fairbank
Phys. Dept. & High Energy
Phys. Laboratory
Stanford University
Stanford, CA 94305

Dr. Anne-Marie Fauchet
Brookhaven National Laboratories
Associated Universities, Inc.
Upton, L.I., NY 11973

Dr. J. Feinstein
Dept. of Electrical Engineering
Stanford University
Stanford, CA 94305

Dr. Frank S. Felber
11011 Torreyana Road
San Diego, CA 92121

Dr. D. Feldman
Los Alamos National Laboratory
P. O. Box 1663
Los Alamos, NM 87545

Dr. Renee B. Feldman
Los Alamos National Laboratory
P. O. Box 1663
Los Alamos, NM 87545

Dr. L. A. Ferrari
Queens College
Department of Physics
Flushing, NY 11367

Dr. C. Finfgeld
ER-542, GTN
Department of Energy
Washington, DC 20545

Dr. A. S. Fisher
Dept. of Electrical Engineering
Stanford University
Stanford, CA 94305

Dr. R. G. Fleig
Hughes Research Laboratory
3011 Malibu Canyon Road
Malibu, CA 90265

Dr. H. Fleischmann
Cornell University
Ithaca, NY 14850

Dr. E. Fontana
Dept. of Electrical Engineering
Stanford University
Stanford, CA 94305

Dr. Norwal Fortson
University of Washington
Department of Physics
Seattle, WA 98195

Dr. Roger A. Freedman
Quantum Institute
University of California
Santa Barbara, CA 93106

Dr. Lazar Friedland
Dept. of Eng. & Appl. Science
Yale University
New Haven, CT 06520

Dr. Walter Friez
Air Force Avionics Laboratory
AFWAL/AADM-1
Wright/Paterson AFB, OH 45433

Dr. Shing F. Fung
Code 696
GSFC
NASA
Greenbelt, MD 20771

Dr. R. Gajewski
Div. of Advanced Energy Projects
U. S. Dept of Energy
Washington, DC 20545

Dr. H. E. Gallagher
Hughes Research Laboratory
3011 Malibu Canyon Road
Malibu, CA 90265

Dr. James J. Gallagher
Georgia Tech. EES-EOD
Baker Building
Atlanta, GA 30332

Dr. W. J. Gallagher
Boeing Aerospace Co.
P. O. Box 3999
Seattle, WA 98124

Dr. J. Gallardo
Quantum Institute
University of California
Santa Barbara, CA 93106

Dr. E. P. Garate
Dept. of Physics and Astronomy
Dartmouth College
Hanover, NH 03755

Dr. A. Garren
Lawrence Berkeley Laboratory
University of California, Berkeley
Berkeley, CA 94720

Dr. Richard L. Garwin
IBM, T. J. Watson Research Ctr.
P.O. Box 218
Yorktown Heights, NY 10598

Dr. J. Gea-Banacloche
Dept. of Physics & Astronomy
Univ. of New Mexico
800 Yale Blvd. NE
Albuquerque, NM 87131

DR. R. I. Gellert
Spectra Technology
2755 Northup Way
Bellevue, WA 98004

Dr. T. V. George
ER-531, GTN
Department of Energy
Washington, DC 20545

Dr. Edward T. Gerry, President
W. J. Schafer Associates, Inc.
1901 N. Fort Myer Drive
Arlington, VA 22209

Dr. Roy Glauber
Physics Department
Harvard University
Cambridge, MA 02138

Dr. B. B. Godfrey
Mission Research Corporation
1720 Randolph Road, S. E.
Albuquerque, NM 87106

Dr. John C. Goldstein, X-1
Los Alamos Natl. Scientific Lab.
P.O. Box 1663
Los Alamos, NM 87545

Dr. Yee Fu Goul
Plasma Physics Lab., Rm 102
S.W. Mudd
Columbia University
New York, NY 10027

Dr. C. Grabbe
Department of Physics
University of Iowa
Iowa City, Iowa 52242

Dr. V. L. Granatstein
Dept. of Electrical Engineering
University of Maryland
College Park, MD 20742

Dr. D. D. Gregoire
Quantum Institute and Dept. of Physics
University of California
Santa Barbara, CA 93106

Dr. Y. Greenzweig
Quantum Inst. and Dept. of Physics
University of California
Santa Barbara, CA 93106

Dr. Morgan K. Grover
R&D Associates
P. O. Box 9695
4640 Admiralty Highway
Marina Del Rey, CA 90291

Dr. A. H. Guenter
Air Force Weapons Laboratory
Kirtland AFB, NM 87117

Dr. K. Das Gupta
Physics Department
Texas Tech University
Lubbock, TX 79409

Dr. Benjamin Haberman
Associate Director, OSTP
Room 476, Old Exe. Office Bldg.
Washington, D.C. 20506

Dr. R. F. Hagland, Jr.
Director, Vanderbilt University
Nashville, TN 37235

Dr. K. Halbach
Lawrence Berkeley Laboratory
University of California, Berkeley
Berkeley, CA 94720

Dr. P. Hammerling
La Jolla Institute
P.O. Box 1434
La Jolla, CA 92038

Dr. R. Harvey
Hughes Research Laboratory
3011 Malibu Canyon Road
Malibu, CA 90265

Prof. Herman A Haus
Mass. Institute of Technology
Rm. 36-351
Cambridge, MA 02139

Dr. S. Hawkins
Lawrence Livermore National Laboratory
P. O. Box 808
Livermore, CA 94550

Dr. Carl Hess
MS B-118
VARIAN
611 Hanson Way
Palo Alto, CA 94303

Dr. J. L. Hirshfield (2 copies)
Yale University
Mason Laboratory
400 Temple Street
New Haven, CT 06520

Dr. K. Hizanidis
Physics Dept.
University of Maryland
College Park, MD 20742

Dr. A. H. Ho
Dept. of Electrical Engineering
Stanford University
Stanford, CA 94305

Dr. Darwin Ho
L-477
Lawrence Livermore National Laboratory
P. O. Box 808
Livermore, CA 94550

Dr. J. Hoffman
Sandia National Laboratories
ORG. 1231, P.O. Box 5800
Albuquerque, NM 87185

Dr. R. Hofland
Aerospace Corp.
P. O. Box 92957
Los Angeles, CA 90009

Dr. Fred Hopf
Optical Sciences Building, Room 602
University of Arizona
Tucson, AZ 85721

Dr. Heinrich Hora
Iowa Laser Facility
University of Iowa
Iowa City, Iowa

Dr. J. Y. Hsu
General Atomic
San Diego, CA 92138

Dr. H. Hsuan
Princeton Plasma Physics Lab.
James Forrestal Campus
P.O. Box 451
Princeton, NJ 08544

Dr. James Hu
Quantum Inst. and Phys. Dept.
University of California
Santa Barbara, CA 93106

Dr. Benjamin Hubberman
Associate Director, OSTP
Rm. 476, Old Executive Office Bldg.
Washington, DC 20506

Dr. J. Hyman
Hughes Research Laboratory
3011 Malibu Canyon Road
Malibu, CA 90265

Dr. H. Ishizuka
University of California
Department of Physics
Irvine, CA 92717

Dr. A. Jackson
Lawrence Berkeley Laboratory
University of California, Berkeley
Berkeley, CA 94720

Dr. S. F. Jacobs
Optical Sciences Center
University of Arizona
Tucson, AZ 85721

Dr. Pravin C. Jain
Asst. for Communications Tech.
Defense Communications Agency
Washington, DC 20305

Dr. E. T. Jaynes
Physics Department
Washington University
St. Louis, MO 63130

Dr. B. Carol Johnson
Ctr. for Radiation Research
National Bureau of Standards
Gaithersburg, MD 20899

Dr. Bernadette Johnson
Lincoln Laboratory
Lexington, MA 02173

Dr. Richard Johnson
Physics International
2700 Merced St.
San Leandro, CA 94577

Dr. G. L. Johnston
NW 16-232
Mass. Institute of Tech.
Cambridge, MA 02139

Dr. Shayne Johnston
Physics Department
Jackson State University
Jackson, MS 39217

Dr. William Jones
U. S. Army SDC
P. O. Box 1500
Huntsville, Al 35807-3801

Dr. R. A. Jong
Lawrence Livermore National Laboratory
P. O. Box 808/L626
Livermore, CA 94550

Dr. Howard Jory (3 copies)
Varian Associates, Bldg. 1
611 Hansen Way
Palo Alto, CA 94303

Dr. C. Joshi
University of California
Los Angeles, CA 90024

Dr. Paul Kennedy
Rockwell International/Rocketdyne Div.
6633 Canoga Avenue, FA-40
Canoga Park, CA 91304

Dr. R. Kennedy
Boeing Aerospace Company
P.O. Box 3999
Seattle, WA 98124

Dr. K. J. Kim, MS-101
Lawrence Berkeley Lab.
Rm. 223, B-80
Berkeley, CA 94720

Dr. I. Kimel
Creol-FEL Research Pavillion
Suite 400
12424 Research Parkway
Orlando, FL 32826

Dr. Brian Kincaid
Lawrence Berkeley Laboratory
University of California, Berkeley
Berkeley, CA 94720

Dr. S. P. Kno
Polytechnic Institute of NY
Route 110
Farmingdale, NY 11735

Dr. Xu Knogyi
Room 36-285
Mass. Institute of Technology
Cambridge MA 02139

Dr. A. Kolb
Maxwell Laboratories, Inc.
8835 Balboa Avenue
San Diego, CA 92123

Dr. Eugene Kopf
Principal Deputy Assistant
Secretary of the Air Force (RD&L)
Room 4E964, The Pentagon
Washington, D.C. 20330

Dr. P. Korn
Maxwell Laboratories, INc.
8835 Balboa Avenue
San Diego, CA 92123

Dr. S. Krinsky
Nat. Synchrotron Light Source
Brookhaven National Laboratory
Upton, NY 11973

Prof. N. M. Kroll
Department of Physics
B-019, UCSD
La Jolla, CA 92093

Dr. Thomas Kwan
Los Alamos National Scientific
Laboratory, MS608
P. O. Box 1663
Los Alamos, NM 87545

Dr. Jean Labacqz
Stanford University
SLAC
Stanford, CA 94305

Dr. Ross H. Labbe
Rockwell International/Rocketdyne Div.
6633 Canoga Avenue, FA-40
Canoga Park, CA 91304

Dr. Willis Lamb
Optical Sciences Center
University of Arizona
Tucson, AZ 87521

Dr. H. Lancaster
Lawrence Berkeley Laboratory
University of California, Berkeley
Berkeley, CA 94720

Dr. D. J. Larson
The Inst. for Accelerator Physics
Department of Physics
University of Wisconsin-Madison
Madison, WI 53706

Dr. J. LaSala
Physics Dept.
U. S. M. A.
West Point, NY 10996

Dr. Bernard Laskovski
M.S. 230-3
NASA-Ames
Moffett Field, CA 94305

Dr. Charles J. Lasnier
TRW
High Energy Physics Lab.
Stanford University
Stanford, CA 94305

Dr. Michael Lavan
U.S. Army Strategic Def. Command
ATTN: Code CSSD-H-D
P. O. Box 1500
Huntsville, AL 35807-3801

Dr. Ray Leadabrand
SRI International
333 Ravenswood Avenue
Menlo Park, CA 94025

Dr. Kotik K. Lee
Perkin-Elmer
Optical Group
100 Wooster Heights Road
Danbury, CT 06810

Dr. K. Lee
Los Alamos Nat. Scientific Lab.
Attn: X-1 MS-E531
P. O. Box 1663
Los Alamos, NM 87545

Dr. Barry Leven
NISC/Code 20
4301 Suitland Road
Washington, D.C. 20390

Dr. B. Levush
Dept. of Physics & Astronomy
University of Maryland
College Park, MD 20742

Dr. Lewis Licht
Department of Physics
Box 4348
U. of Illinois at Chicago Cir.
Chicago, IL 60680

Dr. M. A. Lieberman
Dept. EECS
Univ. of Cal. at Berkeley
Berkeley, CA 94720

Dr. Anthony T. Lin
Dept. of Physics
University of California
Los Angeles, CA 90024

Dr. B. A. Lippmann
Stanford Linear Accel. Center
BIN 26
Stanford, CA 94305

Dr. Chuan S. Liu
Dept. of Physics & Astronomy
University of Maryland
College Park, MD 20742

Dr. R. Lohsen
Los Alamos National Laboratory
P. O. Box 1663
Los Alamos, NM 87545

Dr. D. D. Lowenthal
Spectra Technology
2755 Northup Way
Bellevue, WA 98004

Dr. A. Luccio
Brookhaven National Laboratory
Accelerator Dept.
Upton, NY 11973

Dr. A. Lumpkin
Los Alamos National Laboratory
P. O. Box 1663
Los Alamos, NM 87545

Dr. Phil Mace
W. J. Shafer Assoc.,Inc.
1901 N. Fort Myer Drive
Arlington, VA 22209

Dr. Siva A. Mani
Science Applications Intl. Corp.
1040 Waltham Street
Lexington, MA 02173-8027

Dr. J. Mark
Lawrence Livermore National Lab.
Attn: L-477
P. O. Box 808
Livermore, CA 94550

Dr. T. C. Marshall
Applied Physics Department
Columbia University
New York, NY 10027

Dr. Xavier K. Maruyama
Dept. of Physics
Naval Postgraduate School
Monterey, CA 93943

Dr. Neville Marzwell
Jet Propulsion Lab.
MS 198-330
4800 Oak Grove Drive
Pasadena, CA 91109

Dr. A. Maschke
TRW
Mail Stop 01-1010
1 Space Park
Redondo Beach CA 90278

Dr. Joseph Mathew
Sachs/Freeman Associates
14300 Gallant Fox Lane
Bowie, MD 20715

Dr. K. Matsuda
GA Technologies Inc.
P.O. Box 85608
San Diego, CA 92138

Dr. John McAdoo
Mission Research Corporation
5503 Cherokee Ave., Suite 201
Alexandria, Va 22312

Dr. D. B. McDermott
Electrical Engineering Dept.
University of California
Los Angeles, CA 90024

Dr. J. K. McIver
Dept. of Physics & Astronomy
Univ. of New Mexico
800 Yale Blvd. NE
Albuquerque, NM 87131

Dr. C. McKinstrie
MS B258
P.O. Box 1663
Los Alamos, NM 87545

Col J. F. McNulty
Ground Based Laser Proj. Office
DASD-H-F
White Sands Missile Range, NM 88002-11

Dr. B. McVey
Los Alamos National Laboratory
P. O. Box 1663
Los Alamos, NM 87545

Dr. John Meson
DARPA
1400 Wilson Boulevard
Arlington, VA 22209

Col Thomas Meyer
DARPA/STO
1400 Wilson Boulevard
Arlington, VA 22209

Dr. F. E. Mills
Fermilab
P.O., Box 500
Batavia, IL 60510

Dr. D. R. Mize
Hughes Research Laboratory
3011 Malibu Canyon Road
Malibu, CA 90265

Dr. Mel Month
Brookhaven National Laboratories
Associated Universities, Inc.
Upton, L.I., NY 11973

Dr. B. N. Moore
Austin Research Assoc.
1901 Rutland Dr.
Austin, TX 78758

Dr. Gerald T. Moore
University of New Mexico
Albuquerque, NM 87131

Dr. Warren Mori
1-130 Knudsen Hall
U.C.L.A.
Los Angeles, CA 90024

Dr. Philip Morton
Stanford Linear Accelerator Center
P.O. Box 4349
Stanford, CA 94305

Dr. Jesper Munch
TRW
One Space Park
Redondo Beach, CA 90278

Dr. James S. Murphy
National Synchrotron Light Source
Brookhaven National Laboratory
Upton, NY 11975

Dr. J. Nation
Cornell University
Ithaca, NY 14850

Dr. R. Neighbours
Physics Department
Naval Postgraduate School
Monterey, CA 93943

Dr. George Neil
TRW
One Space Park
Redondo Beach, CA 90278

Dr. Kelvin Neil
Lawrence Livermore National Lab.
Code L-321, P.O. Box 808
Livermore, CA 94550

Dr. W. M. Nevins
L-639
Lawrence Livermore National Laboratory
P. O. Box 808
Livermore, CA 94550

Dr. Brian Newnam
MSJ 564
Los Alamos National Scientific Lab.
P.O. Box 1663
Los Alamos, NM 87545

Dr. W. Nexsen
Lawrence Livermore National Laboratory
P. O. Box 808
Livermore, CA 94550

Lt. Rich Nielson/ESD/INK
Hanscomb Air Force Base
Stop 21, MA 01731

Dr. Milton L. Noble (2 copies)
General Electric Company
G. E. Electric Park
Syracuse, NY 13201

Dr. K. O'Brien
Div. 1241 SNLA
Albuquerque, NM 87185

Dr. John D. O'Keefe
TRW
One Space Park
Redondo Beach, CA 90278

Dr. T. Orzechowski
L-436
Lawrence Livermore National Lab.
P. O. Box 808
Livermore, CA 94550

Prof. E. Ott (2 copies)
Department of Physics
University of Maryland
College Park, MD 20742

OUSDRE (R&AT)
Room 3D1067, The Pentagon
Washington, D.C. 20301

Dr. A. J. Palmer
Hughes Research Laboratory
3011 Malibu Canyon Road
Malibu, CA 90265

Dr. Robert B. Palmer
Brookhaven National Laboratories
Associated Universities, Inc.
Upton, L.I., NY 11973

Dr. J. Palmer
Hughes Research Laboratory
Malibu, CA 90265

Dr. Richard H. Pantell
Stanford University
Stanford, CA 94305

Dr. Dennis Papadopoulos
Astronomy Department
University of Maryland
College Park, Md. 20742

Dr. P. Parks
GA Technologies
P.O. Box 85608
San Diego, Ca 92138

Dr. John A. Pasour
Mission Research Laboratory
8560 Cinderbed Road
Suite 700
Newington, VA 22122

Dr. C. K. N. Patel
Bell Laboratories
Murray Hill, NJ 07974

Dr. Richard M. Patrick
AVCO Everett Research Lab., Inc.
2385 Revere Beach Parkway
Everett, MA 02149

Dr. Claudio Pellegrini
Brookhaven National Laboratory
Associated Universities, Inc.
Upton, L.I., NY 11973

Dr. D. E. Pershing
Mission Research Corporation
5503 Cherokee Avenue
Alexandria, VA 22312

Dr. J. M. Peterson
Lawrence Berkeley Laboratory
University of California, Berkeley
Berkeley, CA 94720

Dr. M. Piestrup
Adelphi Technology
13800 Skyline Blvd. No. 2
Woodside, CA 94062

Dr. Alan Pike
DARPA
1400 Wilson Boulevard
Arlington, VA 22209

Dr. Hersch Pilloff
Code 421
Office of Naval Research
Arlington, VA 22217

Dr. A. L. Pindroh
Spectra Technology
2755 Northup Way
Bellevue, WA 98004

Dr. D. J. Pistoresi
Boeing Aerospace Company
P. O. Box 3999
Seattle, WA 98124-2499

Dr. Peter Politzer
General Atomic Tech., Rm. 13/260
P. O. Box 85608
San Diego, CA 92138

Major Donald Ponikvar
U. S. Army SDC
P. O. Box 15280
Arlington, VA 22245-0280

Dr. S. E. Poor
Lawrence Livermore National Laboratory
P. O. Box 808
Livermore, CA 94550

Prof. M. Porkolab
NW 36-213
Mass. Institute of Technology
Cambridge, MA 02139

Dr. R. V. Pound
Physics Department
Harvard University
Cambridge, MA 02138

Mr. J. E. Powell
Sandia National Laboratories
ORG. 1231, P.O. Box 5800
Albuquerque, NM 87185

Dr. Mark A. Prelas
Nuclear Engineering
Univ. of Missouri-Columbia
1033 Engineering
Columbia, Missouri 65211

Dr. Donald Prosnitz
Lawrence Livermore National Lab.
Attn: L-470
P. O. Box 808
Livermore, CA 94550

Dr. D. C. Quimby
Spectra Technology
2755 Northup Way
Bellevue, WA 98004

Dr. Paul Rabinowitz
Xexon Research and Eng. Comp.
P. O. Box 45
Linden, NJ 07036

Dr. G. Ramian
Quantum Institute
University of California
Santa Barbara, CA 93106

Dr. L. Ranjun
Dept. of Physics
University of Cal. at Irvine
Irvine, CA 92717

Dr. L. L. Reginato
Lawrence Livermore National Laboratory
P. O. Box 808
Livermore, CA 94550

Dr. M. B. Reid
Dept. of Electrical Engineering
Stanford University
Stanford, CA 94305

Dr. D. A. Reilly
AVCO Everett Research Lab.
Everett, MA 02149

Dr. M. Reiser
University of Maryland
Department of Physics
College Park, MD 20742

Dr. S. Ride
Arms Control
Stanford University
Stanford, CA 94305

Dr. C. W. Roberson
Code 412
Office of Naval Research
800 N. Quincy Street
Arlington, VA 22217

Dr. B. Robinson
Boeing Aerospace Company
P.O. Box 3999
Seattle, WA 98124

Dr. K. Robinson
Spectra Technology
2755 Northup Way
Bellevue, WA 98004

Dr. D. Rogers
Lawrence Livermore National Laboratory
P. O. Box 808
Livermore, CA 94550

Dr. Jake Romero
Boeing Aerospace Company
P. O. Box 3999
Seattle, WA 98124-2499

Dr. T. Romesser
TRW, Inc.
One Space Park
Redondo Beach, Ca 90278

Dr. Marshall N. Rosenbluth
Institute for Fusion Studies
The Univ. of Texas at Austin
Austin, TX 78712

Dr. J. B. Rosenzweig
The Inst. for Accelerator Physics
Department of Physics
University of Wisconsin-Madison
Madison, WI 53706

Dr. J. Ross
Spectra Technology
2755 Northup Way
Bellevue, WA 98004

Dr. N. Rostoker
University of California
Department of Physics
Irvine, CA 92717

Dr. G. A. Saenz
Hughes Research Laboratory
3011 Malibu Canyon Road
Malibu, CA 90265

Dr. Antonio Sanchez
Lincoln Laboratory
Mass. Institute of Tech.
Room B213
P. O. Box 73
Lexington, MA 02173

Dr. Aldric Saucier
BMD-PO
Ballistic Missile Defense
Program Office
P. O. Box 15280
Arlington, VA 22215

Dr. A. Saxman
Los Alamos National Scientific Lab.
P. O. Box 1663, MSE523
Los Alamos, NM 87545

Dr. J. Scharer
ECE Dept.
Univ. of Wisconsin
Madison, WI 53706

Dr. E. T. Scharlemann
L626
Lawrence Livermore National Laboratory
P. O. Box 808
Livermore, CA 94550

Prof. S. P. Schlesinger
Dept. of Electrical Engineering
Columbia University
New York, NY 10027

Dr. Howard Schlossberg
AFOSR
Bolling AFB
Washington, D.C. 20332

Dr. George Schmidt
Stevens Institute of Technology
Physics Department
Hoboken, NJ 07030

Dr. M. J. Schmitt
Los Alamos National Laboratory
P. O. Box 1663
Los Alamos, NM 87545

Dr. Stanley Schneider
Rotodyne Corporation
26628 Fond Du Lac Road
Palos Verdes Peninsula, CA 90274

Dr. N. Schoen
TRW DSSG
One Space Park
Redondo Beach, CA 90278

Dr. M. L. Scott
Los Alamos National Laboratory
P. O. Box 1663
Los Alamos, NM 87545

Dr. Richard L. Schriever (DP-23)
Director, Office of Inertial Fusion
U. S. Department of Energy
Washington, D.C. 20545

Dr. R. W. Schumacher
Hughes Research Laboratories
3011 Malibu Canyon Road
Malibu, CA 90265

Dr. H. Schwettmann
Phys. Dept. & High Energy
Physics Laboratory
Stanford University
Stanford, CA 94305

Dr. Marlan O. Scully
Dept. of Physics & Astronomy
Univ. of New Mexico
800 Yale Blvd. NE
Albuquerque, NM 87131

Dr. S. B. Segall
KMS Fusion
3941 Research Park Dr.
P.O. Box 1567
Ann Arbor, MI 48106

Dr. Robert Sepucha
DARPA
1400 Wilson Boulevard
Arlington, VA 22209

Prof. P. Serafim
Northeastern University
Boston, MA 02115

Dr. A. M. Sessler
Lawrence Berkeley Laboratroy
University of California
1 Cyclotron Road
Berkeley, CA 94720

Dr. W. Sharp
L-626
Lawrence Livermore National Laboratory
P. O. Box 808
Livermore, CA 94550

Dr. Earl D. Shaw
Bell Laboratories
600 Mountain Avenue
Murray Hill, NJ 07974

Dr. J. P. Sheerim
KMS Fusion
P.O. Box 1567
Ann Arbor, MI 48106

Dr. R. Shefer
Science Research Laboratory
15 Ward Street
Somerville, MA 02143

Dr. R. L. Sheffield
Los Alamos National Laboratory
P.O. Box 1663
Los Alamos, NM 87545

Dr. Shemwall
Spectra Technology
2755 Northup Way
Bellevue, WA 98004

Dr. Shen Shey
DARPA/DEO
1400 Wilson Boulevard
Arlington, VA 22209

Dr. D. Shoffstall
Boeing Aerospace Company
P.O. Box 3999
Seattle, WA 98124

Dr. I. Shokair
SNLA, Org. 1271
Albuquerque, NM 87185

Dr. J. S. Silverstein
Harry Diamond Laboratories
2800 Powder Mill Road.
Adelphi, MD 20783

Dr. Jack Slater
Spectra Technology
2755 Northup Way
Bellevue, WA 98004

Dr. Kenneth Smith
Physical Dynamics, Inc.
P.O. Box 556
La Jolla, CA 92038

Dr. Lloyd Smith
Lawrence Berkeley Laboratory
University of California
1 Cyclotron Road
Berkeley, CA 94720

Dr. Stephen J. Smith
JILA
Boulder, CO 80302

Dr. T. Smith
TRW, Inc.
One Apace Park
Redondo Beach, CA 90278 R1/2044

Dr. Todd Smith
Hansen Labs
Stanford University
Stanford, CA 94305

Dr. Joel A. Snow, M.S. E084
Senior Technical Advisor
Office of Energy Research
U. S. Department of Energy
Washington, D.C. 20585

Dr. J. Z. Soln (22300)
Harry Diamond Laboratories
2800 Powder Mill Road
Adelphi, MD 20783

Dr. G. Spalek
Los Alamos National Laboratory
P. O. Box 1663
Los Alamos, NM 87545

Dr. Richard Spitzer
Stanford Linear Accelerator Center
P.O. Box 4347
Stanford, CA 94305

Mrs. Alma Spring
DARPA/Administration
1400 Wilson Boulevard
Arlington, VA 22209

SRI/MP Reports Area G037 (2 copies)
ATTN: D. Leitner
333 Ravenswood Avenue
Menlo Park, CA 94025

Dr. W. Stein
Los Alamos National Laboratory
P. O. Box 1663
Los Alamos, NM 87545

Dr. L. Steinhauer
STI
2755 Northup Way
Bellevue, WA 98004

Dr. Efrem J. Sternbach
Lawrence Berkeley Laboratory
University of California, Berkeley
Berkeley, CA 94720

Dr. M. Strauss
Department of Physics
University of California at Irvine
Irvine, CA 92717

Dr. W. C. Stwalley
Iowa Laser Facility
University of Iowa
Iowa City, Iowa 52242

Dr. R. Sudan
Lab. of Plasma Studies
Cornell University
Ithaca, NY 14850

Dr. P. W. Sumner
Hughes Research Laboratory
3011 Malibu Canyon Road
Malibu, CA 90265

Dr. David F. Sutter
ER 224, GTN
Department of Energy
Washington, D.C. 20545

Dr. Abraham Szoke
ML/L-470
Lawrence Livermore Natl. Lab.
P.O. Box 808
Livermore, CA 94550

Dr. R. Taber
Dept. of Phys. & High Energy Lab.
Stanford University
Stanford, CA 94305

Dr. T. Tajima
IFS
Univ. of Texas
Austin, TX 78712

Dr. H. Takeda
Los Alamos National Laboratory
P. O. Box 1663
Los Alamos, NM 87545

Dr. J. J. Tancredi
Hughes Aircraft Co.
Electron Dynamics Division
3100 West Lomita Blvd.
Torrance, CA 90509

Dr. Milan Tekula
AVCO Everett Research Lab.
2385 Revere Beach Parkway
Everett, MA 02149

Dr. R. Temkin (2 copies)
Mass. Institute of Technology
Plasma Fusion Center
Cambridge, MA 02139

Dr. L. Thode
Los Alamos National Laboratory
P. O. Box 1663
Los Alamos, NM 87545

Dr. Keith Thomassen, L-637
Lawrence Livermore National Laboratory
P. O. Box 808
Livermore, CA 94550

Dr. Harold Thompson
TRW, Inc.
R1/2120
One Space Park
Redondo Beach, Ca 90278

Dr. Norman H. Tolk
Physics Department
Vanderbilt University
Nashville, TN 37240

Dr. Kang Tsang
Science Applications Intl. Corp.
10260 Campus Point Drive
San Diego, CA 92121

Dr. E. Tyson
Boeing Aerospace Company
P.O. Box 3999
Seattle, WA 98124

Dr. H. S. Uhm
Naval Surface Warfare Center
White Oak Lab.
Silver Spring, MD 20903-5000

Dr. L. Ulstrup
TRW, Inc.
One Space Park
Redondo Beach, Ca 90278

Under Secretary of Defense (R&D)
Office of the Secretary of Defense
Room 3E1006, The Pentagon
Washington, D.C. 20301

Dr. L. Vahala
Physics Dept.
College of William & Mary
Williamsburg, VA 23185

Dr. A. Valla
Spectra Technology
2755 Northup Way
Bellevue, WA 98004

Dr. A. Vetter
Boeing Aerospace Company
P.O. Box 3999
Seattle, WA 98124

Dr. A. A. Vetter
Spectra Technology
2755 Northup Way
Bellevue, WA 98004

Dr. G. Vignola
Brookhaven National Laboratories
Associated Universities, Inc.
Upton, L.I., NY 11973

Dr. S. A. Von Laven
KMS Fusion Inc.
Ann Arbor, MI 48106

Dr. John E. Walsh
Wilder Laboratory
Department of Physics (HB 6127)
Dartmouth College
Hanover NH 03755

Dr. W. M. Walsh, Jr.
Bell Laboratories
600 Mountain Avenue
Room 1-D 332
Murray Hill, NJ 07974

Dr. Jiunn-Ming Wang
Brookhaven National Laboratories
Associated Universities, Inc.
Upton, L.I., NY 11973

Dr. T-S. Wang
Los Alamos National Laboratory
P. O. Box 1663
Los Alamos, NM 87545

Dr. J. F. Ward
University of Michigan
Ann Arbor, MI 48109

Dr. E. Warden
Code PDE 106-3113
Naval Electronics Systems Command
Washington, DC 20363

Dr. Roger W. Warren
Los Alamos National Sciencific Lab.
P.O. Box 1663
Los Alamos, NM 87545

Dr. J. Watson
Los Alamos National Laboratory
P. O. Box 1663
Los Alamos, NM 87545

Dr. B. Weber
Harry Diamond Laboratories
2800 Powder Mill Road
Adelphi, MD 20783

Dr. Lee Webster
BMD/ATC
Box 1500
Huntsville, AL 35807

Dr. J. T. Weir
Lawrence Livermore National Laboratory
P. O. Box 808
Livermore, CA 94550

Dr. R. Whitefield
15260 Dickens Ave.
San Jose, CA 95124

Ms. Bettie Wilcox
Lawrence Livermore National Lab.
ATTN: Tech. Info. Dept. L-3
P.O. Box 808
Livermore, CA 94550

Dr. Mark Wilson
National Bureau of Standards
Bldg. 245, Rm. B-119
Gaithersburg, MD 20899

Dr. H. Winick
Stanford Synch Rad. Lab.
SLAC Bin 69
P.O. Box 44349
Stanford, CA 94550

Dr. J. Workman
Berkeley Research Associates
P.O. Box 241
Berkeley, CA 94701

Dr. Jack Wong (L-71)
Lawrence Livermore National Lab.
P. O. Box 808
Livermore, CA 94550

Dr. Thomas P. Wright
Sandia National Laboratories
ORG. 1231, P.O. Box 5800
Albuquerque, NM 87185

Dr. J. Wurtele
M.I.T.
NW 16-234
Plasma Fusion Center
Cambridge, MA 02139

Dr. Ming Xie
Dept. of Physics
Stanford University
Stanford, CA 94305

Dr. Yi-Ton Yan
MS-B259
Los Alamos National Lab.
Los Alamos, NM 87545

Dr. A. Yariv
California Institute of Tech.
Pasadena, CA 91125

Dr. J. Yeh
Allied Corporation
31717 La Tienda Dr.
Westlake Village, CA 91362

Dr. A. Yeremian
Boeing Aerospace Company
P.O. Box 3999
Seattle, WA 98124

Dr. Barbara Yoou
R & D Associates
1401 Wilson Blvd., Suite 500
Arlington, VA 22209

Dr. Li Hua Yu
725B, NSLS
Brookhaven National Laboratory
Upton, NY 11973

Dr. Simon S. Yu
Lawrence Livermore National Laboratory
P. O. Box 808
Livermore, CA 94550

Dr. Mark Zedikev
103 S. Goodwin
Urbana, IL 61801

Dr. M. S. Zisman
Lawrence Berkeley Laboratory
University of California, Berkeley
Berkeley, CA 94720

Dr. J. Zumdieck
Spectra Technology
2755 Northup Way
Bellevue, WA 98004

Records 1 copy

Cindy Sims Code 2634 1 copy